HHS Public Access

Author manuscript

Nanophotonics. Author manuscript; available in PMC 2017 December 07.

Published in final edited form as:

Nanophotonics. 2017 August ; 6(5): 853–879. doi:10.1515/nanoph-2016-0189.

Advances in antimicrobial photodynamic inactivation at the nanoscale

Nasim Kashef,
Wellman Center for Photomedicine, Massachusetts General Hospital, Boston, MA 02114, USA

Department of Dermatology, Harvard Medical School, Boston, MA 02115, USA

Department of Microbiology, School of Biology, College of Science, University of Tehran, Tehran, Iran

Ying-Ying Huang, and
Wellman Center for Photomedicine, Massachusetts General Hospital, Boston, MA 02114, USA

Department of Dermatology, Harvard Medical School, Boston, MA 02115, USA

Michael R. Hamblin*
Wellman Center for Photomedicine, Massachusetts General Hospital, Boston, MA 02114, USA

Department of Dermatology, Harvard Medical School, Boston, MA 02115, USA

Harvard-MIT Division of Health Sciences and Technology, Cambridge, MA 02139, USA

Abstract

The alarming worldwide increase in antibiotic resistance amongst microbial pathogens necessitates a search for new antimicrobial techniques, which will not be affected by, or indeed cause resistance themselves. Light-mediated photoinactivation is one such technique that takes advantage of the whole spectrum of light to destroy a broad spectrum of pathogens. Many of these photoinactivation techniques rely on the participation of a diverse range of nanoparticles and nanostructures that have dimensions very similar to the wavelength of light. Photodynamic inactivation relies on the photochemical production of singlet oxygen from photosensitizing dyes (type II pathway) that can benefit remarkably from formulation in nanoparticle-based drug delivery vehicles. Fullerenes are a closed-cage carbon allotrope nanoparticle with a high absorption coefficient and triplet yield. Their photochemistry is highly dependent on microenvironment, and can be type II in organic solvents and type I (hydroxyl radicals) in a biological milieu. Titanium dioxide nanoparticles act as a large band-gap semiconductor that can carry out photo-induced electron transfer under ultraviolet A light and can also produce reactive oxygen species that kill microbial cells. We discuss some recent studies in which quite remarkable potentiation of microbial killing (up to six logs) can be obtained by the addition of simple inorganic salts such as the non-toxic sodium/potassium iodide, bromide, nitrite, and even the toxic sodium azide. Interesting mechanistic insights were obtained to explain this increased killing.

***Corresponding author: Michael R. Hamblin**, Hamblin@helix.mgh.harvard.edu.

Keywords

Antimicrobial photodynamic inactivation; photochemical mechanisms; drug delivery nanovehicles; fullerenes; titanium dioxide photocatalysis; potentiation; Drug-resistant microbial cells; nanotechnology-based drug delivery; titania photocatalysis; efflux-pump inhibition

1 Introduction and basics

The discovery of antibiotics in the 1950s was hailed as a medical miracle that transformed the treatment of infectious disease. However, since then bacteria have progressively developed resistance to each new agent that comes along [1]. In 2015, the O'Neill report garnered much international attention when it delivered the alarming forecast that by 2050 (if nothing were done to stem the growth of multi drug resistant bacteria) there would have been 300 million premature deaths that would have cost the world economy $100 trillion [2].

The current worldwide increase in drug-resistant bacteria and the simultaneous decline in efforts by both academic laboratories and pharmaceutical companies toward the discovery of new antibacterial agents to combat-resistant strains pose a serious threat to the treatment of life-threatening infections. Therefore, it is necessary to develop novel non-invasive and non-toxic antimicrobial strategies that act more efficiently and faster than the current antibiotics, and to which pathogens will not easily develop resistance [3]. One promising alternative to current antibiotics is antimicrobial photodynamic inactivation (aPDI).

aPDI is defined as the application of a non-toxic dye known as a photosensitizer (PS), which can be photo-activated with light of an appropriate wavelength in the presence of oxygen to generate cytotoxic reactive oxygen species (ROS) (singlet oxygen and/or free radicals) [4–6].

The aPDI process is characterized by high selectivity, rapid microbial killing, minimal invasiveness, low occurrence of side effects, and allows repetitive application. The process (schematically illustrated in the Jablonsky diagram shown in Figure 1) is initiated when a ground state PS (S_0) absorbs light of an appropriate wavelength and is converted into an electronic excited singlet state (S_1). Many PS molecules in this short-lived state can decay back to the ground state with the emission of light (fluorescence) or heat (internal conversion) [7], but some can also be transformed into a much longer-lived excited triplet state (T_1, T_3). The excited triplet state PS can do one of two things; it can react with molecular oxygen by energy transfer generating singlet oxygen (a process that is termed a type II reaction) or else it can undergo an electron transfer reaction to form PS radical ions that in turn react with oxygen to produce cytotoxic species such as superoxide, hydrogen peroxide, and/or hydroxyl radicals (which is termed a type I reaction). The singlet oxygen or other ROS can cause damage to bacterial cells or other microbes through several mechanisms. These include oxidation of membrane lipids and amino acids in proteins, cross-linking of proteins and oxidative damage to nucleic acids with the subsequent disturbance of the normal functioning of the pathogen [8, 9].

The use of these photochemical reactions to accomplish a therapeutic benefit is called photodynamic therapy (PDT), and its history goes back to the ancient Indians and Egyptians who used light in combination with naturally occurring plant psoralens to treat skin diseases (e.g. vitiligo, leucoderma). In 1900, Oscar Raab, a medical student working with Professor Herman von Tappeiner in Munich, discovered the lethal effect of the combination of light and acridine red dye on paramecia (a type of single-celled microorganism) by chance. He correlated the killing of the paramecia with the strength of light coming through the nearby window. He noted that the type of dyes that could accomplish this feat were all fluorescent [10, 11]. Shortly afterward, von Tappeiner and Jodlbauer discovered the importance of oxygen in these photosensitization reactions; as a result in 1904 the PDT field was established when they introduced the term “photodynamic action” to describe this phenomenon [12].

It has been proposed that the ROS generated by light-activated PS can trigger microbial killing and cell damage via three mechanisms: (a) damage to the cell membrane (or virus envelope); (b) inactivation of essential enzymes and proteins; and/or (c) damage to DNA [5].

The aPDI-induced photo-damage can result in considerable morphological and functional changes in the microbial cells. Functional damage results from loss of enzymatic activities, protein oxidation and formation of protein-protein cross-links, and inhibition of metabolic processes (e.g. DNA synthesis, glucose transport). Morphological alterations include alteration of the mesosome structure. Direct damage to the cell membrane leads to leakage of cellular contents and following inactivation of the membrane transport system [13].

There is a very wide variation in the cellular structure and organization among different classes of microbes. These variations influence the interaction of exogenous PS with different cellular components, and these can affect the effectiveness and the course of action of the aPDI of different pathogens. Differences in the cell walls of Gram-positive and Gramnegative bacteria play an important role in the susceptibility of bacteria to aPDI. Gram-positive bacteria have a thick and porous peptidoglycan layers that surround a cytoplasmic membrane, while Gram-negative bacteria possess an outer membrane, surrounding a thinner peptidoglycan layer, inside which is the cytoplasmic membrane [14, 15]. To perform aPDI, the PS needs to penetrate (or at least bind to) the cell wall of the bacteria and end up in the plasma membrane or in the cytoplasm; however, the membrane barriers of the bacterial cell limit the simple diffusion of PS into the bacterial cytosol [16, 17]. Therefore, aPDI of Gram-positive bacteria is definitely much easier to accomplish than that of Gram-negative bacteria. The cell walls of fungal cells have a structure that is intermediate in permeability between Gram-positive and Gram-negative bacteria. The outer part is a moderately porous layer of β-glucan and mannan polysaccharides. Figure 2 shows a schematic illustration of the three different cell wall structures.

In many environments bacteria exist as a complex, multispecies surface-associated community termed a biofilm. Organisms within biofilms are embedded in a self-produced matrix of extracellular polymeric substance composed of polysaccharides, proteins, lipids, and extracellular DNA. Bacteria that live in a biofilm community possess several advantages, including structural stability, firm adherence to biotic or abiotic surfaces,

increased virulence, and resistance to both antimicrobial therapy and the host immune response [17–19]. See Figure 3 for a schematic representation of the progress of biofilm formation.

It has been shown that bacteria growing as biofilms are more resistant to aPDI compared with their equivalent planktonic forms. The dye concentration and the light dose used for the photoinactivation of biofilms are considerably higher than those required to inactivate planktonic bacterial suspensions [20–22]. In fact, cells growing in biofilms differ from their planktonic counterparts in a number of aspects, such as the cell wall composition, rate of growth, and presence of polysaccharide intercellular adhesin (PIA), which may block both the uptake of the PS and the penetration of light, and thereby reduce the photosensitizing efficiency [23, 24]. Gad et al. [25] suggested that an abundant production of PIA could obstruct the diffusion of the PS through the extracellular matrix, thus reducing the susceptibility of biofilms to photosensitization.

aPDI is also effective against viruses. The structure of the virus plays an important role in effective aPDI. In general, viruses are categorized according to whether the particle is surrounded by a protein sheath or envelope. The viral envelope is a main target for the aPDI process [26]. Lipids and proteins in the envelope are assumed to act as PS binding sites, and protein damage may be the mechanism underlying virus inactivation [27].

Yeasts and fungal pathogens are also variable in their cell envelopes, and their outer cell walls containing mixtures of glucan, mannan, and chitin carbohydrate polymers. This feature makes them inherently more permeable to external substances compared to Gram-negative bacteria, but still less permeable than Gram-positive bacteria [28].

Fungi (and yeasts) are much less susceptible to aPDI killing than bacteria because of the larger size of the fungal (yeast) cell compared to the small bacterial cell. The amount of ROS needed to kill a yeast cell is much greater than that necessary to kill a bacterial cell [21]. A number of studies have investigated the target site in fungi and yeasts during the aPDI process [29–31].

2 Light sources, optics, and dosimetry

2.1 Light sources

It is a fundamental principle of PDT that the wavelength of the light source should in general be tuned to the absorption maximum of the PS. Longer wavelengths are strongly preferred over shorter wavelengths for *in vivo* applications (see below). Wavelengths that have been used for PDT include ultraviolet A (UVA) (330–400 nm), blue (400–490 nm), green (490–550 nm), yellow (550–600 nm), red (600–700 nm), and near infrared (NIR) (700–810 nm).

For instance, it can be seen from Figure 4 that porphyrins (in particular) have relatively large Soret bands (around 400 nm) and a progressively diminishing set of Q bands, until the last Q-band is reached in the 630 nm region that is extremely weak. If one was employing a porphyrin to carry out aPDI (as is very common in fact), would it make more sense to excite the porphyrin with blue light (400 nm) or with red light (630 nm) or indeed with white light?

However, other tetrapyrrole backbones have been developed with red-shifted absorption maxima such as chlorins (650 nm), phthalocyanines (700 nm), and bacteriochlorins (780 nm). These long wavelengths display much better tissue penetration than shorter wavelengths. All these different backbones have been modified to produce highly active antimicrobial PS. Moreover, many *in vitro* studies have used relatively simple broadband white light (400–700 nm) from an incandescent lamp. All the wavelengths mentioned above are based on one-photon absorption by the PS. However, in recent years non-linear processes, such as two-photon absorption, have been studied to mediate PDT [32, 33]. The idea here is that if two long wavelength photons 750–1000 nm arrive at the PS molecule at virtually the same time (within 1 ps), they will both be absorbed and it will be as if a single photon with half the wavelength was absorbed instead. The advantage is that the long wavelength photons pass much better through tissue than the equivalent (1/2 λ) photons with shorter wavelength. Recently, two-photon PDT with graphene quantum dots (QDs) was used to kill both Gram-positive and Gram-negative bacteria [34].

When PDT became a clinically employed modality (in the 1970s), it was common to use a laser as the light source. The monochromatic nature of the light and the focused and collimated beam made coupling the light into fiber-optic cables relatively easy. More recently, light-emitting diodes (LEDs) have become popular due to their advantages of being safe, inexpensive, and easy to operate. Organic LEDs are yet another more recent advance with advantages of flexibility [35]. In a similar vein, we have the recent introduction of light-emitting fabrics, which can be made into wearable light-emitting clothing, and is currently being used clinically for PDT of actinic keratoses on the scalp [36]. The advantages of these wearable light sources are as follows. They allow the total light source to be delivered over a much longer time span, and at a much lower power density (mW/cm^2). This means that one of the main limitations of PDT (exhaustion of the available oxygen supply) can be overcome by reducing the rate of consumption of oxygen and allowing its resupply to occur by natural diffusion [37, 38]. Another advantage of using low power densities for longer times is that the pain of treatment is markedly lower (pain can be a limiting factor in dermatologic PDT) [39].

2.2 Light delivery and dosimetry

It is well known that living tissue both absorbs and scatters incident visible light. Both absorption and scattering decrease as the wavelength of the light increases. Moreover, different tissue types (arising from different organ systems) can have very different optical properties. The standard optical properties that govern light penetration into tissue are categorized as follows: the reduced absorption coefficient; the reduced scattering coefficient; and the anisotropy factor (the degree to which light is forward scattered) [40].

The difficulties that light has in penetrating into tissue have led to a range of technologies being developed to deliver light deep within the body. Many organ systems that develop malignant or infectious lesions are connected to the outside by hollow tubes such as esophagus, trachea/bronchus, intestine, or urethra. Sophisticated endoscopes have been developed to transport light deep within the body [41].

Recently, the ability to introduce fiber-optic diffusers through the skin (transdermally) and allow direct light delivery to lesions deep within the body via interstitial fibers has been developed [42]. This technology has built upon groundwork that was originally developed for introduction of radioactive brachytherapy seeds into cancers such as prostate cancer. There are template grids with needles that can accept optical fibers introduced into the tissue, combined with imaging and software designed to ensure predictable and even coverage of light intensity over a defined three-dimensional volume of internal tissue [43]. The third novel advance in light delivery inside the body is the idea of wirelessly powered implantable LED light sources [44]. These were originally developed for optogenetic applications, which require long-term delivery of blue light into the brains of mice and rats [45]. Nevertheless, these devices would be equally applicable for PDT with red or NIR light.

2.3 Photosensizer delivery and dosimetry

There is a big difference between PDT for cancers and for infections when it comes to the route of PS delivery [46]. By far the best way to deliver the PS to cancers is to inject the compounds intravenously. For water-insoluble compounds, this route is likely to require a delivery vehicle such as liposomes or micelles [47]. However, for infections, the best way to deliver the PS is locally, either by topical application or by instillation. The reason for this difference is that the binding of the PS to microbial cells is rapid and mediated mainly by charge-charge interactions, while the uptake of the PS by cancer cells is slower and is more likely to be mediated by hydrophobic interactions. Therefore, one important method of encouraging high selectivity of aPDI for microbial cells over surrounding host mammalian cells is to employ local delivery and a short-drug light interval. Since the majority of PSs are very fluorescent, it is common to carry out quantitative fluorescent imaging to confirm that there is a sufficient accumulation of PS in the target lesion [48].

When light is delivered to the PS and ROS are generated, one phenomenon that is frequently observed is that the ROS attack the very molecule responsible for their photogeneration, i.e. the PS itself. This process is known as photobleaching, and is often used as a surrogate marker for PDT effectiveness. Photobleaching is usually measured by monitoring the fluorescence of the PS with increasing doses of activating light [49]. However, it is sometimes the case that when treating an infection in an experimental animal with PDT, it becomes necessary to add an additional amount of PS, in order to replace the PS that has been destroyed by photobleaching [50].

3 Photodynamic inactivation and nanotechnology

An ideal PS designed for aPDI should possess a wide range of properties including a high quantum yield of singlet oxygen or other photochemical reaction product, be a pure compound with a stable composition, soluble in water, selective to the target tissue (or cells), safe, and non-toxic for normal healthy cells [51]. However, many PS, such as porphyrins, chlorins, and phthalocyanines, are highly lipophilic and tend to aggregate in the aqueous environment in physiological conditions, resulting in the loss of photosensitizing activity [52]. So, one of the most important problems in PDI is optimizing drug delivery of the PS. Several studies have reported suitable PS carriers that can improve PS delivery, e.g.

liposomes [53, 54], micelles [55], and nanoparticles (NPs) [56–58] (schematically illustrated in Figure 5).

NPs, with dimensions generally in the 1–200 nm range, are able to pass through many biological barriers, enabling their cargos to gain access to critical molecules and biological systems, thus improving drug availability at the target area to provide the maximum therapeutic benefit. In the field of nanomedicine, nano-sized materials are used that can be engineered as delivery vehicles to carry various therapeutic or diagnostic agents and can be potentially useful for medical applications [59]. NPs can be divided into composition that are either naturally occurring or synthetic in origin, and then sub-divided into organic (carbon containing) or inorganic. Subsequent classification is generally based on morphology (spherical, tube, etc.) or structure (vesicle, hollow, solid) and components such as metals, metal oxides, lipids, proteins, and nucleic acids that are important to their function [60].

The use of nanotechnology for enhancing delivery of PS is an attractive approach to improving aPDI. This goal may be achieved in different ways, for instance by enhancing the delivery of the PS to microorganisms (encapsulating the PS in NPs) or by increasing the $^1O_2$ yield of the PS (by covalently binding the PS to the surface of the NPs, or simply by mixing the NPs and PS together). In some cases, the NPs themselves (for instance, TiO_2, fullerenes, or QDs) have been shown to act as PS themselves and are capable of photodynamically inactivating microorganisms.

3.1 PSs contained inside self-assembled NPs (liposomes or micelles)

Liposomes are spherical nano-sized vesicles made from a self-assembled lipid bilayer formed from natural phospholipids and cholesterol. Liposomes are the most widely studied colloidal carrier system that can be loaded with PSs with the goal to solubilize, deliver, and transport them to a specific target, thus preventing the drug from degradation as well as limiting adverse effects from non-targeted drug [61]. Liposomes are mainly made of one or more concentric phospholipid bilayers each unit of which consists of an inner hydrophilic head and outer hydrophobic tail. The hydrophobic center of these bilayers can accommodate hydrophobic PSs, while the hydrophilic central region or core can accommodate water-soluble PSs [62, 63]. In this manner PSs can be encapsulated into liposomes due to the lipophilicity and water solubility of the PS itself.

Liposomes are most commonly employed to encapsulate lipophilic PSs and have been proved to improve the aPDI of various PSs, not only because liposomes enhance the solubility and stability of PSs, but also because they can facilitate the penetration of PSs into bacteria by means of fusion processes or disturbing the cell walls [53, 54, 64].

The use of polymeric micelles as vehicles of PSs is another promising approach for aPDI [55, 65]. The polymeric micelle delivery system may improve drug solubility and prevent the formation of aggregates in the aqueous medium. Compared to the use of liposomes, preparation of polymeric micelles can be much less expensive and simpler.

3.2 PS embedded in NPs (polymeric or mesoporous silica)

NPs loaded with a PS have been used as carriers to deliver the PS into microorganisms and improve antimicrobial performance; particular attention has been placed on biocompatible and biodegradable matrices such as silica because the application of aPDI is likely to be in the medical arena (wounds, or localized infections) or environmental situations (food industry, water purification).

Many different functional groups can be added to the surface of silica nanoparticles (SiNPs). These SiNPs serve as a potential carrier for aPDI applications [66]. SiNPs can be prepared with well-controlled particle size, shape, porosity, and monodisperse distribution. In addition, several different PSs can be encapsulated, SiNPs are stable to pH changes, and are not subject to microbial attack. Due to the permeability of the porous matrix to molecular oxygen, singlet oxygen that is generated inside can come out, so the photo-destructive effect can be maintained in an encapsulated form [67].

3.3 PS bound to the surface of NPs (metals such as gold or silver)

PSs have been covalently bound to the surface of NPs to prepare a new PS with better properties than the original PS; this is the main difference of this approach compared to the previous PS encapsulation, which is an improved delivery method. In order to bind the PS to the NP surface, both the PS and the NP surface have to display some reactive groups where the linking can occur. The second step is the reaction between the functionalized group on the NP surface and the PS [68].

Gold nanoparticles (AuNPs) have been used in two ways in PDT: first, as drug-delivery platforms in a similar manner to other inorganic NPs [69]; second, as surface plasmon-enhanced agents taking account of the non-linear optical fields associated with very close distances to metal NPs [70] (Figure 6). The AuNPs have good biocompatibility, versatile surfaces, and unique optical properties [71]. Figure 6A shows a PS attached to the outer surface of AuNPs. Figure 6B shows how the local optical field can be dramatically enhanced by the surface-plasmon resonance especially in certain geometries such as ring shaped [72] (or nanostars) [73]. In Figure 6C the PDT effect of AuNP-bound PS can be enhanced by plasmon resonance.

AuNPs, in combination with PSs, have been employed to achieve greater microbial killing through aPDI [74–76]. Sherwani et al. [74] investigated the photodynamic effect of AuNP-conjugated methylene blue (MB) (Figure 7A) or toluidine blue (Figure 7B) against *Candida albicans* biofilm. They also examined the photodynamic efficacy of PS-conjugated AuNPs to treat skin and oral *C. albicans* infection in BALB/c mice. Their results showed that the AuNPs-PS conjugate-based aPDI was found to effectively kill both *C. albicans* planktonic cells and biofilm populating hyphal forms. The mixture of AuNPs conjugated to two different PSs significantly depleted the hyphal *C. albicans* burden against superficial skin and oral *C. albicans* infection in mice.

Tawfik et al. [75] also evaluated the photodynamic effect of MB-AuNPs conjugate on *Staphylococcus aureus*, which were isolated from impetigo lesions. The highest significant

inhibitory effect on *S. aureus* was obtained with MB-AuNPs conjugate when irradiated by a diode laser 660 nm. The percentage of viable bacteria was 3%.

Silver is known to be an antimicrobial agent due to the high affinity of Ag toward the sulfur and phosphorus atoms in biomolecules [77]. AgNPs can react with sulfur containing amino acids in the cell membrane that will affect cell viability, and can also react with sulfur containing moieties inhibiting enzyme function involved in DNA replication [78–80] causing cell death [81]. The antimicrobial effects of AgNPs against both Gram-positive and Gram-negative bacteria have been shown to be dependent on the dose [82, 83], particle size [84, 85], total surface area [86, 87], and the particle shape [88]. The antimicrobial effect of silver is dependent on superficial contact [89].

Most of the scientific literature on the toxicology of AgNPs toward both microbial cells and mammalian cells has only been published in the past decade [90–92]. Many of these studies have revealed AgNPs to have noticeable toxicity against several cell lines as well as a number of aquatic organisms, but the mechanistic basis of these toxic effects is now an area of active research. In particular, the bioavailability of silver ions (Ag^+) from AgNPs, considered by many as a major factor in Ag-mediated toxicity, remains poorly understood [93, 94]. For example, certain algal species are more sensitive to AgNPs than to free Ag^+, but the addition of cysteine (known to form complexes with Ag^+) reduces the toxic effects of both Ag sources [95].

Ivask et al. [96] for the first time investigated the size-dependent toxic effects of a well-characterized library of AgNPs against several microbial species, protozoans, algae, crustaceans, and mammalian cells *in vitro*.

In spite of the antimicrobial properties of AgNPs, microbial synthesis of these NPs has been proposed as one of the alternative eco-friendly green methods to chemical and physical procedures that are full of problems including the use of toxic solvents, generation of hazardous by-products, and high energy consumption [97]. Many microorganisms have been used for intra- or extra-cellular biosynthesis of AgNPs [98–102].

Silver-containing environmental surfaces and textiles in health care settings are increasingly promoted as products that may help reduce health-care associated infections (HAIs) by reducing microbial loads as demonstrated in laboratory studies or environmental microbiological testing [103]. There have been some innovative attempts to prepare antibacterial paints by incorporating silver NPs using various composite materials [104–106]. However, no evidence as yet demonstrates that these products actually help reduce HAIs.

Misba et al. [107] evaluated the anti-biofilm efficacy of aPDI by conjugating toluidine blue O (TBO) with silver AgNPs. *Streptococcus mutans* was exposed to laser light in the presence of TBO-AgNPs conjugate. The results showed a reduction in the viability of bacterial cells by 4 $\log_{10}$. The crystal violet assay, confocal laser scanning microscopy, and scanning electron microscopy revealed that the TBO-AgNPs conjugates inhibited biofilm formation, increased the uptake of propidium iodide, and leakage of the cellular constituents, respectively.

3.4 NPs themselves act as the PS

There are some instances when the NPs themselves act as the PS in the absence of preformed PS [67]. In this case, the NPs themselves have to be able to absorb light by virtue of possessing an extinction coefficient of appreciable size in an appropriate region of the electromagnetic spectrum and to form an excited state that can lead to some photochemical generation of ROS. Examples of these classes of NPs include fullerenes, titanium dioxide (TiO_2), QDs, and even upconversion nanoparticles (UCNPs).

3.4.1 Fullerenes—The fullerene molecules have a unique structure entirely composed of sp2 hybridized carbon atoms arranged in a soccer ball structure [108]. Their molecular diameter is at the lower end of the NP scale, but they have very high photo-stability and are able to act as PS in aPDI, as the triplet state of the fullerene molecule has a very high triplet yield and a long triplet lifetime that can interact with molecular oxygen [109]. Their disadvantage is their absorption spectrum, which is disposed toward the blue and green visible wavelengths rather than the red/far-red wavelengths that have good tissue penetration. Huang et al. [110] showed that cationic fullerenes have a good selectivity for binding to microbial cells compared with mammalian cells and can be studied in antimicrobial applications. Other reports have also studied the role of fullerenes as PS in aPDI [111–114].

In the field of nanomedicine, the medical applications of fullerenes are gathering more attention in both the therapeutic and diagnostic fields. Fullerenes are a unique class of pure carbon allotropes characterized by symmetric closed cages of sp2 hybridized carbon atoms forming a combination of either five-member or six-member rings on the cage surface. For example, fullerene C60 possesses a geometrical shape in which 60 carbon atoms are arranged as a truncated icosahedron with 32 faces (12 pentagonal and 20 hexagonal) and 60 vertices [115]. C60 is the most abundant component in commonly prepared mixtures of fullerenes, and has been the most studied over the last few decades compared to other fullerenes, such as C70 and C84 [116].

Due to their extended system of π-conjugation, fullerenes have large absorption coefficients in the visible and UV spectral regions. Moreover, they have a high triplet quantum yield allowing them to catalyze photodynamic reactions. It has been observed that fullerenes, either in their pristine form or in their functionalized form, can catalyze the formation of ROS after illumination. Just like the classic tetrapyrrole PS used for PDT, the illumination of fullerenes (dissolved in organic solvents and in the presence of molecular oxygen) leads to the generation of highly reactive singlet oxygen, due to an energy transfer from the excited triplet state of the fullerene. Nevertheless, many studies show that the illumination of fullerenes in polar solvents (especially in water), and in the presence of reducing agents such as a reduced form of nicotinamide adenine dinucleotide (NADH), will generate type II ROS, such as superoxide anions and hydroxyl radicals [109].

Fullerenes can offer some advantages as photosensitizing agents over conventional PS with a typical tetrapyrrole structure, including their higher photostability (less photo-bleaching), their possibility to be modified by chemical functionalization (to obtain the desired degree of hydrophilicity), the possibility of attaching light-harvesting antennae onto the fullerenes (to

increase the quantum yield of reactive species). Moreover, fullerenes can self-assemble into nano-vesicles called fullerosomes, which can act as drug delivery vehicles with different targeting properties. In contrast, a major disadvantage of fullerenes is their relatively poor absorption in the red or far-red regions of the visible spectrum, because their main absorption bands occur in the UV, blue, and green regions. But this drawback could be overcome in many ways, such as the attachment of light-harvesting antennae, which absorb in the red wavelengths [117] or the use of two-photon excitation [118, 119].

Fullerenes can efficiently photo-inactivate pathogenic microbial cells, especially when suitable functional groups have been introduced into the fullerene cage structure. It seems that the mechanism involved in destroying the bacteria and other pathogens involves attacking biomolecules in the pathogen structure with superoxide anions, singlet oxygen, and free radicals.

As mentioned above, functionalization of fullerenes can influence on aPDI effectiveness. Tegos et al. [120] reported functionalized C60 with hydrophilic and cationic groups, and tested these derivatives for aPDI. The fullerene derivatives with polar diserinol and quaternary pyrrolidinium groups were the most efficient in killing micro-organisms on light irradiation. Huang et al. [117] showed that increasing the number of positive charges on fullerenes could improve their efficiency. They used water-soluble decacationic fullerenes aiming to eradicate Gram-positive and Gram-negative bacteria. These researchers confirmed that PSs with greater numbers of cationic charges are more efficient for aPDI, and concluded that for the elimination of Gram-positive bacteria, singlet oxygen is necessary, while reactive hydroxyl radicals are needed for significant damage to Gram-negative bacteria.

Mizuno et al. [112] also investigated the importance of the number of cationic charges on the photodynamic efficiency of fullerene derivatives in aPDI. These researchers used a series of functionalized cationic fullerenes as PSs, comparing the aPDI efficacy of synthetic fullerene derivatives that presented either basic or quaternary amino groups against *S. aureus*, *Escherichia coli*, and *C. albicans*. Their results showed that the most effective fullerene derivatives on aPDI were tetracationic derivatives (BF21, see Figure 7E), in particular against *S. aureus*. The *E. coli* results were intermediate and *C. albicans* was the most aPDI-resistant species tested.

A unique class of water-soluble fullerene adducts, decacationic methano-fullerene decaiodides C60 [>M(C_3N_6 + C_3)$_2$]-(I^-)$_{10}$[1-(I^-)$_{10}$] was reported by Wang et al. [121, 122]. These compounds when excited with both UVA light and white light were capable of generating $^1O_2$ (type II) and also highly reactive hydroxyl radicals formed from superoxide, via a type I photochemical reaction. The authors designed the 10 quaternary ammonium cationic charges per C60 cage to boost the ability of the fullerene to target Gram-positive (>6 logs of killing) and Gram-negative bacteria (2.5 logs of killing) using white light.

Aoshima et al. [123] also studied the antimicrobial photodynamic activities of fullerene C60 and its derivatives against both bacteria and fungi. They used water-soluble fullerenes encapsulated into carriers (polyvinylpyrrolidone/C60, gammacyclodextrin (gamma-CD)/C60, and nano-C60) and three types of fullerenols (C60 $(OH)_{12}$, C60 $(OH)_{36}$•$8H_2O$, and

C60 $(OH)_{44}$•$8H_2O$). The fullerenols displayed good antimicrobial activity against *Propionibacterium acnes, Staphylococcus epidermidis, C. albicans*, and *Malassezia furfur*. In addition, the results showed that the activity of fullerenols against fungi was stronger than against bacteria. The authors indicated that fullerenols are more water-soluble and could interact more with components such as β-glucan and chitin in fungus cell wall than with peptidoglycan in the bacterial cell membrane.

Huang et al. [124] investigated the aPDI of pathogenic bacteria by novel water-soluble decacationic fullerene monoadducts, C60[> M(C3N6(+)C3)2], and C70[> M(C3N6(+)C3)2]. In the presence of a high number of electron-donating iodide anions as parts of quaternary ammonium salts in the arm region, they found that C70[> M(C3N6(+)C3)2] produced more highly reactive hydroxyl radical than C60[> M(C3N6(+)C3)2], in addition to singlet oxygen. They suggested to kill Gram-positive and Gram-negative bacteria by C60[> M(C3N6(+)C3)2] and C70[> M(C3N6(+)C3)2], respectively. The hypothesis is that singlet oxygen can diffuse more easily into porous cell walls of Gram-positive bacteria to reach sensitive sites, while the less permeable Gram-negative bacterial cell wall needs the more reactive hydroxyl to cause real damage.

In another study, the photodynamic mechanism of action induced by N,N-dimethyl-2-(4′-N,N,N-trimethylaminophenyl)fulleropyrrolidinium iodide (DTC60 (2+)) was investigated on *C. albicans* and *E. coli* cells [125]. Photogeneration of superoxide anion radical by DTC60 (2+) in the presence of NADH was detected using nitro blue tetrazolium method in reverse micelles. In *C. albicans* suspensions, 10 μM DTC60 (2+) was an effective PS, producing an ~5 log decrease of cell survival when the cultures were irradiated for 30 min with visible light. Also, *C. albicans* cell growth was not detected in the presence of 10 μM DTC60 (2+) and irradiation. Photodynamic mechanism investigations were compared in both *C. albicans* and *E. coli* cells. Studies under anoxic conditions indicated that oxygen was required for the PDI of these microorganisms. The photocytotoxicity induced by DTC60 (2+) was similar in D_2O than in water cell suspensions. Furthermore, photo-inactivation of microbial cells was negligible in the presence of azide ion, while the addition of mannitol produced a photo-protective effect on the cellular survival. These results indicated that DTC60 (2+) has potential as an agent to the PDI of microbial cells. Also, the photo-cytotoxicity activity induced by this cationic fullerene derivative can involve the intermediacy of both superoxide anion radical and singlet molecular oxygen.

It is well known that enveloped viruses can be efficiently eliminated by singlet oxygen-generating compounds, such as photodynamic agents. A wide variety of PSs have demonstrated good potential for viral inactivation, i.e. phthalocyanines, merocyanines, porphyrin derivatives, hypericin (HY) (Figure 7D), Rose Bengal (RB) (Figure 7C), and MB.

At present, there is one method using PSs for the inactivation of viruses that is allowed to be used in the production of blood plasma components for pathogen reduction. This procedure consists of the treatment of fresh-frozen blood plasma with MB and visible light, reducing the viral activity without damaging plasma proteins [126]. However, this method is not indicated for labile blood products such as packed erythrocytes or thrombocytes, and MB has the disadvantage of remaining in the plasma after the treatment. Therefore, fullerenes

could be an alternative to classical PSs for blood product decontamination. Kasermann and Kempf [127] used the singlet-oxygen-generating agent C60 because it can be quickly removed from aqueous solutions and suspensions such as blood plasma. The authors used viruses from two different families: Togaviridae (Semliki Forest Virus) and Rhabdoviridae (Vesicular Stomatitis Virus). The viral particles were suspended in buffered solutions containing C60, and this suspension was then illuminated with visible light for up to 5 h, resulting in a loss of infectivity of more than 7 logs in viral titers. This viral inactivation was demonstrated to be oxygen dependent and equally efficient in solutions containing proteins as found in plasma. Two additional advantages can be noted concerning the use of fullerenes for viral inactivation: their insolubility in aqueous solutions, and their extreme stability. Thus, heterogeneous C60 can be easily removed from the incubation medium by simple procedures such as centrifugation, filtration, or by the introduction of special properties (e.g. magnetism) into the fullerenes cages. The removal of C60 from the solutions is desirable in order to help to reduce any toxic effects or undesirable consequences that may arise from the use of this PS in biological fluids. In addition, its high stability makes it possible for C60 to be recycled (an economic advantage).

3.4.2 TiO_2—TiO_2 is capable of mediating photo-oxidation, and can produce ROS on light absorption by electron transfer reactions involving oxygen and water. It seems that the active species is mainly hydroxyl radical (HO·), but superoxide anion and $^1O_2$ are also produced [128–130] (see Figure 8).

The main problem to the use of TiO_2-NPs for medical applications is that their absorption is basically in the UV region of the electromagnetic spectrum. Researchers have focused on shifting the absorbance spectrum of TiO_2 toward the visible region through doping with other elements [131, 132]

TiO_2 has been widely studied as a PS in a process termed “photocatalysis”, which has been proposed as an antimicrobial strategy for disinfecting wastewater [133]. Photocatalysis is the acceleration of a light-mediated reaction in the presence of a catalyst (usually an inorganic semi-conductor). The advantage of photocatalysis is having sunlight or UV radiation to trigger the disinfection process using a catalyst (TiO_2) [134].

Photocatalysis, the acceleration of a light-mediated reaction in the presence of a catalyst (usually an inorganic semiconductor) [135], is a rapidly growing technology that is being investigated for applications in solar energy conversion [136] and for environmental remediation and disinfection [137, 138]. Antimicrobial photocatalysis describes a process in which semiconductor NPs such as TiO_2 are irradiated with sunlight or UVA to generate ROS in order to kill various types of microorganisms [135, 139–143]. The procedure of antimicrobial photocatalysis has most often been suggested to be used in water purification [143].

TiO_2 is a wide band-gap, n-type semiconductor, with the characteristics of low toxicity, strong optical absorption, low cost, and high chemical stability. The active form of TiO_2 is the NP form and it has allowed it to be incorporated into paints, films, and a host of different materials that can be made “self-sterilizing”. A variety of medical applications of TiO_2

photocatalysis have been suggested, among which are self-sterilizing urinary catheters [144], self-sterilizing lancet for blood glucose determination [145], antibacterial food packaging film [146], antibacterial dental implants [147], and antibacterial surgical implants [148].

The advantages of antimicrobial photocatalysis (as compared to other kinds of photodynamic inactivation) are as follows:

1. It is a heterogeneous system so the solid TiO_2 could be removed from the reaction after use.
2. The TiO_2 is not easily photo-bleached in the same way as organic PSs are photo-bleached by light delivery.
3. TiO_2 can be activated by UVA wavelengths present in natural sunlight making the process suitable for remediation of contaminated wastes in outdoor settings.

Nevertheless, there is a need to improve the efficiency of TiO_2 antimicrobial catalysis. Researchers are trying to dope the TiO_2 with platinum or nitrogen or other materials in order to shift the activation wavelength away from the UV to the visible range [149] and to fabricate different types of titania nanostructures such as TiO_2 nanotubes [150]. A commonly employed form of TiO_2 NPs is called P25 Degussa (Evonik) that is commercially available and has been reported to be composed of about 75% of the anatase crystalline isoform [151].

3.4.3 QDs—QDs are semiconductor NPs, which have several characteristics that make them a potentially new class of PS. These small NPs (size range of 1–6 nm) have high quantum yields, a constant composition, high photo-stability, and fluorescent emission properties that can be tunable by size. They are relatively simple and inexpensive to synthesize, are non-cytotoxic in the absence of light, but have the potential to induce cytotoxicity under UV irradiation [152]. They can be targeted to specific pathological areas and made water soluble. QDs can transfer energy to surrounding oxygen, in a similar manner to traditional PS. Recent papers have explored their potential to act as a PS in their own right [153, 154].

QDs have also been examined as enhancers of the efficacy of TBO-aPDI. Enhanced killing was shown to be due to a non-Förster resonance energy transfer mechanism, whereby the QD converted part of the incident light closer to the absorption maximum for TBO; hence more light energy was harvested, resulting in increased concentrations of bactericidal radicals [155].

3.4.4 UCNPs—Lanthanide-doped UCNPs are dilute guest-host systems where trivalent lanthanide ions are dispersed as a guest in an appropriate dielectric host lattice with a dimension of less than 100 nm. The dopants of rare-earth metals exhibit luminescent behavior, and produce emission when excited. Through selection of lanthanide dopants, UCNPs can display wavelength (color) selective upcon-version, such as NIR to shorter NIR, visible (blue, green, red), or UV [156]. The mechanism involves the sequential absorption of two photons via a “virtual intermediate excited state” leading to the emission of light at shorter wavelength than the excitation wavelength (Figure 9).

PDT has been used for therapy in prostate, lung, head and neck, or skin cancers. However, conventional PDT is limited by the penetration depth of visible light needed for its activation [157]. NIR light in the “window of optical transparency” (750–1100 nm) of tissue can penetrate significantly deeper into tissues than the visible light, because absorbance and light scattering for most body constituents are minimal in this range [158]. Importantly, UCNPs can efficiently convert the deeply penetrating NIR light to visible wavelengths that can excite PS to produce cytotoxic $^1O_2$, promising their use in PDT treatment of deeply tumors.

Although the aPDI effect has been demonstrated against viruses, it has been slow in gaining acceptance mainly because of several limitations such as the hydrophobicity of PSs, poor target specificity, and limited tissue penetration ability. Most PSs are hydrophobic and aggregate easily in aqueous solutions, affecting their photochemical and photobiological properties [159]. Many PSs also suffer from poor target specificity, which leads to collateral damage to the healthy cells and tissues. Moreover, current light source used is either UV or short wavelength visible light as most of the PSs absorb at relatively short wavelengths that possess limited tissue penetration ability that restricted the amount of light to be delivered to the target sites.

Lim et al. [160] reported a UCNP-based PDI strategy that could potentially overcome the limitations faced by the current approaches. They designed and synthesized NIR-to-visible UCNPs that consist of sodium yttrium fluoride ($NaYF_4$) nanocrystals co-doped with ytterbium (Yb3þ) and erbium (Er3þ) ions. The UCNPs synthesized were coated with a layer of high molecular weight polyethyleneimine (PEI). The chosen PS molecules, zinc phthalocyanine (ZnPc), were attached onto the surface of NIR-to-visible UCNPs. On exposure to NIR light at 980 nm, the ZnPc-attached UCNPs (ZnPc-UCNPs) emit visible light that is being absorbed by the PSs. The excited PSs then convert nearby molecular oxygen to ROS, resulting in viral inactivation. Using these NPs, they examined the feasibility of this inactivation strategy by inactivating viruses photodynamically in suspension and a murine model. The UCNPs effectively reduced the infectious virus titers *in vitro* with no clear pathogenicity in the murine model and increased target specificity to virus-infected cells.

The findings from this work demonstrated the possibility of UCNP-based PDI to photodynamically inactivate viruses with advantages over the current aPDI technique. By carrying the PS, the ZnPc-UCNPs “solubilize” the highly nonpolar ZnPc. These NPs also mediate the conversion from lower energy radiation to higher energy emission essential to excite the ZnPc. Also, increased target specificity is achievable as the surface of the NPs can be modified with the established protocol for bioconjugation of targeting moieties such as antibodies or proteins.

3.5 Microneedles as an emerging drug delivery technology

In the treatment of chronic wounds, the delivery of photosensitizing agents is often hindered by the presence of a thick hyperkeratotic or a necrotic tissue layer, thus reducing their therapeutic efficacy. Microneedles (MNs) are an emerging drug delivery technology using short sharp projections that can penetrate the outer layers of the skin, without causing any noticeable pain or tissue damage, whilst minimizing damage to the skin barrier function

[161]. MNs are 25–2000 μm in length and are arranged in arrays that can contain up to 2000 needles per square centimeter [162]. Delivering photosensitizing drugs using this platform has been demonstrated to have several advantages over conventional PDT, such as painless application, reduced erythema, enhanced cosmetic results, and improved intra-dermal delivery [163]. For instance, dissolving MNs (Gantrez(R) AN-139 co-polymer) were loaded with MB for carrying out aPDI of *S. aureus, E. coli*, and *C. albicans* biofilms [164].

4 Methods of potentiating aPDI

4.1 Potentiation by inhibition of efflux pumps

Multi-drug efflux pumps (MEPs) are now broadly recognized as the major components of microbial resistance to many classes of antibiotics [165]. Some MEPs selectively expel specific antibiotics, while others, referred to as multidrug resistance pumps, can mediate efflux of a variety of structurally diverse compounds with differing modes of action. Figure 10 shows the five major families of MEPs that occur in bacteria and fungi.

Phenothiazinium-based PSs such as TBO, MB, and azure dyes have been employed in aPDI research for nearly 80 years [166]. Phenothiazinium salts are amphipathic planar molecules that possess one intrinsic quaternary nitrogen atom and have phototoxic efficiency against a broad range of microorganisms, such as *E. coli*, *S. aureus*, streptococci, *Listeria monocytogenes*, and *Vibrio vulnificus* [167–171].

MB has been used as an intrinsic antimicrobial compound in conventional (non-light-mediated) antimicrobial therapy research for over a 100 years [166]. It has been reported that photodynamic activity of MB occurs mostly, via the type I mechanism [172]. Several studies have reported its *in vitro* activity and in animal models of infection, and MB has received regulatory approval to mediate PDT of dental infectious diseases, such as periodontitis and caries [173–175]; however, it seems that MB is not the optimum member of the class of phenothiazinium derivatives for antimicrobial photo-inactivation. Wainwright et al. [176] compared five different phenothiazinium dyes as antibacterial PSs against methicillin-resistant *S. aureus* (MRSA). They found that dimethyl methylene blue (DMMB) and new methylene blue (NMB) were the most active compounds but they had dark toxicity.

In 2006, Tegos and Hamblin showed for the first time that phenothiazinium salts were substrates of MEPs [177]. The MEPs in Gram-positive bacterial species are primarily classified as the major facilitator-type (characterized by NorA in *S. aureus*), while Gram-negative species tend to have three-component MEPs, known as resistance nodulation division (RND) and characterized by MexAB-OprM in *Pseudomonas aeruginosa* [165].

In 2008, Tegos et al. [178] reported that four different inhibitors of the NorA pump (the diphenyl urea INF271, reserpine, 5-methoxyhydnocarpin, and the polyacylated neohesperidoside) significantly potentiated aPDI of *S. aureus* mediated by MB, TBO, and 1,9-DMMB and an inhibitor of Gram-negative RND pumps (phenylalanine-arginine beta-naphthylamide) also potentiated light-mediated killing of *P. aeruginosa* by TBO. The discovery that these efflux pump inhibitors (EPI) had a dramatic effect in potentiating the

killing effect of aPDI with phenothiazinium dyes suggested that EPI may have some clinical application in this field.

Kishen et al. [179] evaluated the ability of MB and RB to inactivate biofilms of *Enterococcus faecalis*. The role of a specific microbial EPI, verapamil hydrochloride, in the MB-mediated aPDI of *E. faecalis* biofilms was also investigated. The results showed that *E. faecalis* biofilms exhibited significantly higher resistance to aPDI when compared with *E. faecalis* in suspension. aPDI with cationic MB produced superior inactivation of *E. faecalis* strains in a biofilm along with significant destruction of biofilm structure when compared with anionic RB. The ability to inactivate biofilm bacteria was further enhanced when the EPI was used with MB. These experiments demonstrated the advantage of MB combined with an EPI to inactivate biofilm bacteria and disrupt biofilm structure.

In another study, Prates et al. [180] investigated whether the major fungal multidrug efflux systems (MESs) affected the efficiency of MB-mediated aPDI in *C. albicans* and tested specific inhibitors of these efflux systems to potentiate aPDI. *C. albicans* wild-type and mutants that over-expressed two classes of MESs [ATP-binding cassette (ABC) and major facilitator superfamily (MFS)] were tested for aPDI using MB as the PS with and without the addition of MES inhibitors. The uptake and cytoplasm localization of PS were achieved using laser confocal microscopy. Their results showed that ABC MES over-expression reduced MB accumulation and aPDI killing more than MFS MES over-expression. Furthermore, by combining MB-aPDI with the ABC inhibitor verapamil, fungal killing and MB uptake were potentiated, while by combining MB-aPDI with the MFS inhibitor INF271, fungal killing and MB uptake were inhibited.

4.2 Potentiation by the addition of inorganic salts

4.2.1 Azide—Huang et al. [181] showed that the addition of sodium azide (NaN_3) paradoxically potentiated aPDI of Gram-negative and Gram-positive bacteria using MB as the PS. In that study, they used two different PS: MB (type I mechanism) and polyethylenimine-chlorin (e6) (PEI-ce6) conjugate (type II mechanism) expecting to see quenching of killing by NaN_3. NaN_3 is well known as a physical quencher of $^1O_2$ [182] and has been widely employed to quench singlet oxygen during aPDI [183]. They observed that addition of NaN_3 (100 μm or 10 mm) to Gram-negative *E. coli* and Gram-positive *S. aureus* incubated with MB and illuminated with red light gave significantly increased bacterial killing (1–3 logs), rather than the expected protection from killing. The other antibacterial PS, PEI-ce6 conjugate, showed reduced aPDI killing (1–2 logs) after the addition of 10 mm NaN_3. Azide (0.5 mm) potentiated bacterial killing by Fenton reagent (hydrogen peroxide and ferrous sulfate) by up to 3 logs, but protected against killing mediated by sodium hypochlorite and hydrogen peroxide (considered to be a chemical source of singlet oxygen). The intermediacy of $N_3^{\bullet}$ radical was confirmed by spin-trapping and electron spin resonance studies in both MB-photosensitized reactions and Fenton reagent with the addition of NaN_3. They found that N_3 radical was formed and bacteria were killed even in the absence of oxygen, suggesting the direct one-electron oxidation of azide anion by photo-excited MB. Although azidyl radicals are less reactive than hydroxyl radicals ($HO^{\bullet}$) or $^1O_2$, they may be more selective and effective bactericidal agents, because they live longer than

$HO^{\bullet}$ radicals. This longer lifetime may be responsible for enhanced aPDI as $N_3^{\bullet}$ radicals may diffuse deeper into the cells and then cause more lethal destruction, while the more reactive $HO^{\bullet}$ or $^1O_2$ is rapidly consumed at the cell wall or in solution [184].

Kasimova et al. [184] attempted to gain deeper understanding of this interesting observation of the potentiation of aPDI by azide. They used six phenothiazinium dyes: MB, TBO, NMB, DMMB, azure A, and azure B. These compounds have varying lipophilicities as measured by the log *p* value (octanol-water partition coefficient). They also compared the Gram-negative bacterial species *E. coli* with a Gram-positive counterpart *S. aureus*, and studied the effect of washing unbound dye out of the bacterial suspension. They found both significant potentiation (up to 2 logs) and also significant inhibition (>3 logs) of killing by adding 10 mm azide depending on Gram classification, washing the dye from the cells, and dye structure. Killing of *E. coli* was potentiated with all six PSs after a wash, while *S. aureus* killing was only potentiated by MB and TBO with a wash and DMMB with no wash. More lipophilic dyes (higher log *p* value, such as DMMB) were more likely to show potentiation. They concluded that potentiation of aPDI by azide (Type I photochemical mechanism) depends on the microenvironment of the PS. The dye is likely to be more tightly bound to the bacterial cells: (a) for more negatively charged Gram-negative bacteria, (b) after a wash to remove unbound dye, and (c) in the case of more lipophilic dyes. When the dye is strongly bound it may be more probable to receive an electron transfer from azide to its triplet-excited state thereby producing a radical pair (PS radical anion and azidyl radical). A complementary hypothesis is that firmly bound dyes can transfer the electron from the PS radical anion into the bacterial cell with its metabolic electron transport chains, thus regenerating the ground state uncharged PS and allowing the process to repeat indefinitely. As non-firmly bound PSs are not adjacent to the bacterial cells, they cannot carry out this secondary electron transfer.

Further research is necessary to see whether azide anion can potentiate microbial killing of other classes of antimicrobial PSs. It should be noted that azide is toxic to both mammalian cells and to microorganisms including bacteria (all Gram-negative but not many Gram-positive species) [185]. Azide inhibits the activity of cytochrome c oxidase in a similar manner to cyanide. Thus, it is clear that the potentiation of aPDI by addition of azide could never be used clinically, but has value as a mechanistic tool to understand the basic photochemistry [184].

Yin et al. [186] investigated the relative abilities of C60[> M(C3N6(+)C3)2]-(I(−))10 (LC14), C60[> CPAF-(MN6(+)C3)2]-(I(−))10 (LC15), and C60[> M(C3N6(+)C3)2] [> M(C3N6C3)2]-(I(−))10 (LC16) to generate singlet oxygen $^1O_2$, hydroxyl radicals ($HO^{\bullet}$), and hydrogen peroxide (H_2O_2) after excitation by UVA or by white light. They used three different classes of pathogenic microbial cells (MRSA, *E. coli*, and *C. albicans*). LC15 was the most powerful broad spectrum antimicrobial fullerenyl photosensitizer followed by LC16, and LC14 was least powerful. Killing depended on both fullerene monoadduct concentration and light fluence. Bacterial killing was not much inhibited by addition of azide anions and in some cases was potentiated. In the absence of oxygen, microbial photokilling was highly potentiated (up to 5 logs) by the addition of azide anions. They concluded that molecular functional addends that encouraged a type I electron-transfer

mechanism increased the ability of photoactivated fullerene monoadducts to kill microbial cells. Oxygen-independent photokilling was possible with fullerene monoadducts in the presence of azide anions, probably mediated by azidyl radicals.

4.2.2 Thiocyanate (SCN^-)—Pseudohalides besides N_3^-, such as thiocyanate (SCN^-), also function as ●OH scavengers [187]. Due to the known reactivity of SCN^- with ●OH and sulfur with $^1O_2$, St Denis et al. [188] wanted to investigate whether SCN^- could potentiate the MB and light-mediated killing of the Gram-positive *S. aureus* and the Gram-negative *E. coli*. SCN^- enhanced aPDI (10 μm MB, 5 J/cm^2 660 nm hv) killing in a concentration-dependent manner of *S. aureus* by 2.5 $\log_{10}$ to a maximum of 4.2 $\log_{10}$ at 10 mm ($p < 0.001$) and increased killing of *E. coli* by 3.6 $\log_{10}$ to a maximum of 5.0 $\log_{10}$ at 10 mm ($p < 0.01$). They determined that SCN^- rapidly depleted O_2 from an irradiated MB system, reacting exclusively with $^1O_2$, without quenching the MB excited triplet state. SCN^- reacted with $^1O_2$, producing a sulfur trioxide radical anion. Their results showed that MB-PDI of SCN^- in solution produced both sulfite and cyanide anions, and that addition of each of these salts separately enhanced MB-PDI killing of bacteria.

4.2.3 Iodide—As sodium azide cannot be used in clinical applications due to its toxicity, Vecchio et al. [189] investigated the effect of the inorganic salt potassium iodide (KI) in combination with aPDI using MB. The safe and effective use of KI was reported in 2001 by the Food and Drug Administration (FDA) [190] and it is commonly used as a clinical antifungal agent [191]. In this study, bacterial killing was tested *in vitro* against *S. aureus* and *E. coli* using MB with KI. They also wanted to confirm that it was possible to increase the efficacy of aPDI by adding KI to MB in an *in vivo* model of localized infection consisting of mouse burn wounds. By adding KI, they observed a reliable increase of red light-mediated bacterial killing of Gram-positive and Gram-negative species *in vitro*. The addition of KI increased in bacterial killing by 4 and 2 logs for *S. aureus* and *E. coli*, respectively. *In vivo*, they also detected less bacterial recurrence in wounds in the days after treatment. On the basis of their results, it seems that the mechanism of the synergistic effect of KI with MB-aPDI producing an increase of bacterial killing involves the generation of short-lived reactive iodine reactive species ($I^●$ or $I_2^●$).

Huang et al. [192] wanted to know whether antimicrobial photocatalysis mediated by TiO_2 could be potentiated by addition of KI and whether the mechanism was via photocatalytic production of iodine/tri-iodide or hypoiodite. Their results showed that addition of the nontoxic inorganic salt KI to TiO_2 (P25) excited by UVA potentiated the killing of Gram-positive bacteria (MRSA), Gram-negative bacteria (*E. coli*), and fungi (*C. albicans*) by up to 6 logs. The microbial killing depended on the concentration of TiO_2, the fluence of UVA light, and the concentration of KI (the best effect was at 100 mm). There was formation of long-lived antimicrobial species (probably hypoiodite and iodine) in the reaction mixture (detected by adding bacteria after light), but short-lived antibacterial reactive species (bacteria present during light) produced more killing. Fluorescent probes for ROS (hydroxyl radical and singlet oxygen) were quenched by iodide. Tri-iodide (which has a peak at 350 nm and a blue product with starch) was produced by TiO_2-UVA-KI but was much reduced when MRSA cells were also present. The model tyrosine substrate N-acetyl tyrosine ethyl

ester was iodinated in a light dose-dependent manner. They concluded that UVA-excited TiO_2 in the presence of iodide produced reactive iodine intermediates during illumination that killed microbial cells and long-lived oxidized iodine products that killed after light has ended.

Zhang et al. [114] synthesized C60-fullerene (LC16) bearing decaquaternary chain and deca-tertiary-amino groups that facilitates electron-transfer reactions via the photoexcited fullerene. Addition of the harmless salt, KI (10 mm) potentiated the UVA or white light-mediated killing of Gram-negative bacteria *Acinetobacter baumannii*, Gram-positive MRSA and fungal yeast *C. albicans* by 1–2 + logs. The mouse model infected with bioluminescent *A. baumannii* gave increased loss of bioluminescence when iodide (10 mm) was combined with LC16 and UVA/white light. They concluded that the mechanism may involve photo-induced electron reduction of (1)(C60 >)* or (3)(C60 >)* by iodide producing I · or I2 followed by subsequent intermolecular electron-transfer events of (C60 >)− to produce reactive radicals.

Freire et al. [193] studied the effects of aPDI on *C. albicans* as biofilms grown *in vitro* and also in an immunosuppressed mouse model of oral candidiasis infection. They used a luciferase-expressing strain that allowed non-invasive monitoring of the infection by bioluminescence imaging. MB and NMB were used as PSs, combined or not with KI, and red laser (660 nm) at four different light doses (10J, 20J, 40J, and 60J). The best *in vitro* log reduction of CFU/ml on biofilm grown cells was: MB plus KI with 40J (2.31 log); and NMB without KI with 60J (1.77 log). These conditions were chosen for treating the *in vivo* model of oral Candida infection. After 5 days of treatment, the disease was practically eradicated, especially using MB plus KI with 40J. Their study suggested that KI can potentiate aPDI of fungal infection using MB (but not NMB) and could be a promising new approach for the treatment of oral candidiasis.

4.2.4 Bromide—For the first time, Wu et al. [194] reported that the addition of sodium bromide to photo-activated TiO_2 potentiated the killing of Gram-negative, Gram-positive bacteria, and fungi by up to 3 logs. The potentiation increased with increasing bromide concentration in the range of 0–10 mm. According to their result, the mechanism of potentiation was probably due to generation of both short- and long-lived oxidized bromine species including hypobromite. There was some antimicrobial activity remaining in solution after switching off the light, that lasted for 30 min but not 2 h, and oxidized 3,3′,5,5′-tetramethylbenzidine. N-Acetyl tyrosine ethyl ester was brominated in a light dose-dependent manner; however, no bromine or tribromide ion could be detected by spectrophotometry or liquid chromatography–mass spectrometry. The mechanism appears to have elements in common with the antimicrobial system (myeloperoxidase + hydrogen peroxide + bromide).

5 aPDI for treating localized infections

5.1 Laboratory animal models of infections

Laboratory experiments conducted with small animals such as rats or mice that have been deliberately infected by various pathogens are the commonest way of testing whether any

aPDI protocol can treat a localized infection. In general, the PS is introduced into the infected lesion, and followed after a relatively short time by light delivery to the infected area [6, 195]. However, if these experiments involve killing of animals at various time points in order to quantify the number of CFUs present in the infected tissues, this tend to be rather laborious and time consuming in order to obtain enough data points to reach statistical significance. This problem was overcome by the Hamblin laboratory, who devised a system of using bioluminescent bacteria and a low-light imaging camera to longitudinally monitor the progress of the infection in real time in a non-invasive manner [196]. This methodology was used in a number of studies that investigated various aspects of aPDI in localized infections in mouse models [197–199].

Tawfik et al. [200] assessed the effect of combining a composite NP composed of MB and AuNPs for aPDI of cutaneous fungal infection in rabbits caused by one of the commonest organisms in onychomycosis that is *Trichophyton mentagrophytes*. PDT was initiated at day 3 to 5 after inoculation, for four sessions 48 h apart. All groups were investigated macroscopically and microscopically (histopathology and scanning electron microscope). Flow cytometry assessment for cell death and X-ray analysis for AuNPs accumulation in brain and liver tissues were also determined. Their results showed that recovery from infection approaching 96% in AuNPs + light group, around 40% in MB-PDT, and 34% in composite PDT. The observed findings confirmed by an apparent decrease of apoptosis; however, small amounts of AuNPs detected in the brain and liver. The animals included in this study showed no behavioral changes, weight loss, or mortality.

One interesting question that is sometimes raised is: why is MB a fairly efficient PS in *in vitro* studies, but *in vivo* its performance can be disappointing. The answer comprises several considerations. First, phenothizinium dyes such as MB can be tricky antimicrobial PS to optimize probably due to a tendency to dimerize and aggregate. Secondly, MB can bind to mammalian cells and tissues. Thirdly, MB can be reduced to the colorless leuko-form by enzymes present in living tissue.

Sherwani et al. [74] also examined the photodynamic efficacy of PS-conjugated AuNPs (AuNPs-PS) to treat skin and oral *C. albicans* infection in BALB/c mice. The biomimetically synthesized AuNPs were conjugated to MB or TBO. The conjugation of PSs with AuNPs was characterized by spectroscopic and microscopic techniques. The therapeutic efficacy of the combination of the AuNP conjugates against cutaneous *C. albicans* infection was examined in a mouse model by enumerating residual fungal burden and histopathological studies. The mixture of AuNPs conjugated to two different PSs significantly depleted the hyphal *C. albicans* burden against superficial skin and oral *C. albicans* infection in mice.

Zhang et al. [114] synthesized C60-fullerene (LC16) bearing decaquaternary chain and decatertiary-amino groups that facilitate electron-transfer reactions via the photo-excited fullerene. They evaluated the effect of LC16 in aPDI of *A. baumannii* infection in mice. The mouse model infected with bioluminescent *A. baumannii* gave increased loss of bioluminescence when KI (10 mm) was combined with LC16 and UVA/white light.

Huang et al. [201] also synthesized a highly water-soluble [70] fullerene monoadduct, C70[> M(C3N6(+) C3)2]-(I(−))10 (LC17), and bisadduct, C70[> M(C3N6(+) C3)2][> M(C3N6C3)2] (LC18), both with a well-defined decacationic quaternary ammonium iodide moiety with 10 positive charges per C70 to give water solubility and bacterial binding. A mouse model of third-degree burn infection with bioluminescent Gram-negative bacteria was used to test the *in vivo* effectiveness of the therapeutic approach using the more effective UVA excitation. Both compounds were effective determined by bioluminescence imaging.

Grinholc et al. [202] examined *in vitro* efficacy of a C60 fullerene functionalized with one methylpyrrolidinium group to kill upon irradiation with white light Gram-negative and Gram-positive bacteria, as well as fungal cells. Using *in vivo* studies, a 2 log10 reduction in the average bioluminescent radiance between treated and non-treated mice was demonstrated. One day after aPDI treatment, moist and abundant growth of bacteria could be observed on wounds of light alone and dark control mice, while aPDI-treated wounds stayed visibly clear up to the third day.

HY is a naturally occurring, potent PS. However, its lipophilicity limits its therapeutic applications. Nafee et al. [203] developed a biodegradable nanocarrier for HY capable of preserving its antibacterial photoactivity. Amphiphilic block copolymers were synthesized to prepare hypericin-laden nanoparticles (HY-NPs). The antimicrobial photoactivity of HY-NPs was assessed *in vivo* on infected wounds in rats. Wound healing studies in rats revealed faster healing, better epithelialization, keratinization, and development of collagen fibers when HY-NPs were applied. Determination of growth factors and inflammatory mediators in the wound area confirmed superior healing potential of nanoencapsu-lated HY.

Lu et al. [111] studied the aPDI activity of a C60 fullerene functionalized with three dimethylpyrrolidinium groups (BF6) *in vivo* on two potentially lethal mouse models of infected wounds. They used stable bioluminescent bacteria and a low-light imaging system to follow the progress of the infection noninvasively in real time. An excisional wound on the mouse back was contaminated with one of two bioluminescent Gram-negative species, *Proteus mirabilis* (2.5×10^7 cells) and *P. aeruginosa* (5×10^6 cells). A solution of BF6 was placed into the wound followed by delivery of up to 180 J/cm^2 of broadband white light (400–700 nm). In both cases there was a light dose-dependent reduction of bioluminescence from the wound not observed in control groups (light alone or BF6 alone). Fullerene-mediated PDT of mice infected with *P. mirabilis* led to 82% survival compared with 8% survival without treatment ($p < 0.001$). PDT of mice infected with highly virulent *P. aeruginosa* did not lead to survival, but when PDT was combined with a suboptimal dose of the antibiotic tobramycin (6 mg/kg for 1 day), there was a synergistic therapeutic effect with a survival of 60% compared with a survival of 20% with tobramycin alone ($p < 0.01$).

5.2 Naturally occurring animal infections

As an intermediate step between experimental studies in laboratory animals, the testing of aPDI on naturally occurring infections is an attractive option [204]. The first study was conducted by Hawkins et al. [205]. These authors investigated the effect of erythrosin B and visible light on third-stage larvae of gastrointestinal nematodes of naturally infected cattle.

Cattle were treated orally with erythrosin B at dosages of 30 and 40 mg/kg/day for as many as 17 days. Feces from treated and untreated animals were collected and prepared for culture. Third-stage larvae were then collected by Baermannization and exposed to light. Both sunlight and artificial fluorescent light were shown to be toxic to third-stage larvae after treatment with erythrosin B. This toxic reaction was significant after only two consecutive daily treatments.

There are other reports indicating the effect of aPDI on the inactivation of pathogens associated with animal infections [206, 207].

Bovine mastitis is considered the most important disease of worldwide dairy industry. Treatment of this disease is based on the application intra-mammary antibiotic, which favors an increase in the number of resistant bacteria in the last decade. Sellera et al. [208] investigated the efficacy of MB-aPDI in the inactivation of pathogens associated with bovine mastitis (*S. aureus, Streptococcus agalactiae, Streptococcus dysgalactiae, Corynebacterium bovis*, and the alga *Prototheca zopfii*). *S. dysgalactiae, S. aureus*, and *C. bovis* were inactivated after 30 s of irradiation, whereas *S. agalactiae* was inactivated after 120 s and *P. zopfii* at 180 s of irradiation. These results showed that aPDI could be an interesting tool for inactivating pathogens for bovine mastitis.

Peri-implantitis is a progressive peri-implant bone loss, which is accompanied by inflammatory lesions in the soft tissues. Hayek et al. [209] compared the effects of aPDI and conventional technique on microbial reduction in ligature-induced peri-implantitis in dogs. Eighteen third premolars from nine Labrador retriever dogs were extracted and the implants were submerged. After osseointegration, peri-implantitis was induced. After 4 months, ligature was removed and natural bacterial plaque was allowed to form for another 4 months. The animals were then randomly divided into two groups. In the conventional group, they were treated using mucoperiosteal flaps for scaling the implant surface and chlorexidine (conventional) irrigation. In the aPDI group, only mucoperiosteal scaling was carried out before PDT. Inside the peri-implant pocket, a paste-based azulene PS was placed and then a GaAlAs low-power laser ($\lambda = 660$ nm, $p = 40$ mW, $E = 7.2$ J for 3 min) was used. Microbiological samples were obtained before and immediately after treatment. Before treatment, one implant was removed and analyzed by scanning electron microscopy to validate the contamination. The results of this study showed that *Prevotella sp., Fusobacterium sp.*, and S. Beta-haemolyticus were significantly reduced for both groups. After treatment, no significant differences were observed between the groups.

Bumblefoot, referring to “bed-sore-like” lesions on the feet, is one of the most important clinical complications in captive birds and has a multi-factorial etiology. Nascimento et al. [210] aimed to compare outcomes in a group of captive penguins, *Spheniscus magellanicus* with bumblefoot lesions treated with aPDI or antibiotics. Ten captive Magellanic penguins with preexisting stage III bumblefoot lesions were selected and randomly divided into one aPDI and one antibiotic group, each including 11 pelvic-limb lesions. In the antibiotic group, antibiotic ointment was applied topically three times a week, and systemic antibiotic and anti-inflammatory drugs were administered daily. In the aPDI group, PDT was applied three times a week without the use of topical or systemic medication. Lesion areas were

photographed, and swabs were collected for culture and sensitivity, on the first day and every 14 days for a total of 84 days. The four species of bacteria showing the most resistance to the antibiotics screened on the antibiogram were used to determine resistance to aPDI with an *in vitro* test. There were significant differences in healing rate and average healing time between the aPDI and antibiotic groups (63.62% vs. 9.09% and 42 vs. 70 days, respectively).

Also, in another study by Sellera et al. [211], five Magellanic penguins with previous pododermatitis lesions on their footpad were treated with PDT. MB (aqueous solution at a concentration of 300 mm) was applied, and after 5 min of incubation in dark to allow microbial uptake the lesion was irradiated using a diode laser, emitting 100 mW at 660 nm of wavelength, distributed in five equidistant points of 0.02 cm^2 that received 140 J/cm^2 each. All PDT-treated lesions successfully regressed and no recurrence was observed during the 6-month follow-up period.

5.3 Clinical infections

aPDI has been successfully applied for elimination of pathogens. The dual selectivity of aPDI (i.e. the selective PS and the localized selective illumination) is an advantage in the treatment of infectious diseases [212]. aPDI was tested as a novel antimicrobial treatment in bacterially colonized chronic leg ulcers and chronic diabetic foot ulcers [213]. Cationic 3,7-bis(di-n-butylamino) phenothiazin-5-ium bromide (PPA904) was used as the PS. The trial included 16 patients with chronic leg ulcers and 16 patients with diabetic foot ulcers (each eight active treatment/eight placebo) in a blinded, randomized, placebo-controlled, single treatment, phase IIa trial. All patients had an ulcer duration of >3 months, bacterially colonized with $>10^4$ CFU/ml. After quantitatively assessing pre-treatment bacterial load via swabbing, PPA904 or placebo was applied topically to wounds for 15 min, followed immediately by 50 J/cm^2 of red light and the wound was again sampled for quantitative microbiology. Wound area was measured for up to 3 months after treatment. The treatment was well tolerated with no reports of pain or other safety issues. In contrast to placebo, patients on active treatment showed a reduction in bacterial load immediately post-treatment ($p < 0.001$). After 3 months, 50% (four out of eight) of actively treated chronic leg ulcer patients showed complete healing compared with 12.5% (one out of eight) placebo patients.

aPDI has been effectively applied for the treatment of cutaneous leishmaniasis (CL), which is caused by parasites of the species Leishmania. Asilian and Davami [214] studied the parasitological and clinical efficacy of aPDI vs. topical paromomycin in patients with Old World CL caused by *Leishmania major* in Iran. Topical paromomycin is one of the many drugs that have been suggested for the treatment of CL caused by Leishmania major. In this clinical trial, 60 patients with the clinical and parasitological diagnosis of CL were recruited and were randomly divided into three treatment groups (weekly topical aPDI, twice-daily topical paromomycin, and placebo, respectively). At the end of the study, complete improvement was seen in 29 of 31 (93.5%), 14 of 34 (41.2%), and 4 of 30 lesions (13.3%) in groups 1, 2, and 3, respectively ($p < 0.001$). At the same time point, 100%, 64.7%, and 20% of the lesions had parasitological cure in groups 1, 2, and 3, respectively ($p < 0.001$).

Periodontal diseases have also been treated successfully by aPDI mediated by conventional PS [215–217]. However, de Freitas et al. [218] investigated the effect of aPDI using MB-loaded poly(lactic-co-glycolic) (PLGA) NPs (MB-NP) in a clinical pilot study with 10 adult human subjects with chronic periodontitis. Patients were treated either with ultrasonic scaling and scaling and root planing (US + SRP) or ultrasonic scaling + SRP + aPDI with MB-NP (25 μg/ml and 20 J/cm^2) in a split-mouth design. The clinical study demonstrated the safety of aPDI. Both groups showed similar improvements of clinical parameters 1 month after treatments. However, at 3 months ultrasonic SRP + aPDT showed a greater effect (28.82%) on gingival bleeding index compared to ultrasonic SRP. The author suggested that the utilization of PLGA NPs encapsulated with MB may be a promising adjunct in antimicrobial periodontal treatment.

6 Conclusions

aPDI can be an alternative or adjunctive treatment modality for infectious diseases. The use of nanotechnology for enhancing delivery of PSs is an attractive approach to improving aPDI. NPs can enhance the PS delivery component, by enabling optimum PS encapsulation, and enhanced uptake within the microbial cells.

In spite of the economic opportunities, nanomedicine faces some serious problems. For instance, their successful commercialization is primarily dependent on their reputation with the general public. Unfortunately, governments, industry, and citizens are poorly informed and prepared for the new health practices [219]. Moreover, there is no coordinated strategy among researchers that addresses the potential risks for human health and the environment [73, 220, 221]. This may endanger the future of a new and promising technology.

The biological activity and biokinetics depend on size, shape, chemistry, and surface properties of the nanomaterials. These variables are likely to modify responses and cell interactions, and could induce toxicity [222]. Toxicity issues are of particular concern but are often ignored. Therefore, it is essential that fundamental research be carried out to address these issues if successful efficient application of these technologies is going to be achieved.

Acknowledgments

MRH was funded by US NIH R01AI050875. NK was supported by the University of Tehran.

References

1. Tenover FC, McGowan JE Jr. Reasons for the emergence of antibiotic resistance. Am J Med Sci. 1996; 311:9–16. [PubMed: 8571988]
2. O’Neill J. Tackling a global health crisis: initial steps. The Review on Antimicrobial Resistance Chaired by Jim O’Neill. 2015
3. Taylor PW, Stapleton PD, Paul Luzio J. New ways to treat bacterial infections. Drug Discov Today. 2002; 7:1086–91. [PubMed: 12546840]
4. Hamblin MR. Antimicrobial photodynamic inactivation: a bright new technique to kill resistant microbes. Curr Opin Microbiol. 2016; 33:67–73. [PubMed: 27421070]
5. Hamblin MR, Hasan T. Photodynamic therapy: a new antimicrobial approach to infectious disease? Photochem Photobiol Sci. 2004; 3:436–50. [PubMed: 15122361]

6. Huang L, Dai T, Hamblin MR. Antimicrobial photodynamic inactivation and photodynamic therapy for infections. Methods Mol Biol. 2010; 635:155–73. [PubMed: 20552347]
7. Green TJ, Wilson DF, Vanderkooi JM, DeFeo SP. Phosphorimeters for analysis of decay profiles and real time monitoring of exponential decay and oxygen concentrations. Anal Biochem. 1988; 174:73–9. [PubMed: 3218748]
8. Ochsner M. Photophysical and photobiological processes in the photodynamic therapy of tumours. J Photochem Photobiol B. 1997; 39:1–18. [PubMed: 9210318]
9. Luksiene Z. Photodynamic therapy: mechanism of action and ways to improve the efficiency of treatment. Medicina (Kaunas). 2003; 39:1137–50. [PubMed: 14704501]
10. Raab O. Uber die Wirkung fluoreszierender Stoffe auf Infusorien. Z Biol. 1900; 39:524–46.
11. Von Tappenier H. Uber die Wirkung fluoreszierender Stoffe auf Infusorien nach Versuchen von O. Raab Muench Med Wochenschr. 1900; 47:5.
12. Von Tappeiner H, Jodlbauer A. Uber Wirkung der photodyna-mischen (fluorieszierenden) Stoffe auf Protozoan und Enzyme. Dtsch Arch Klin Med. 1904; 80:427–87.
13. Jori G, Fabris C, Soncin M, et al. Photodynamic therapy in the treatment of microbial infections: basic principles and perspective applications. Lasers Surg Med. 2006; 38:468–81. [PubMed: 16788934]
14. Bourré L, Giuntini F, Eggleston IM, Mosse CA, Macrobert AJ, Wilson M. Effective photoinactivation of Gram-positive and Gram-negative bacterial strains using an HIV-1 Tat peptide-porphyrin conjugate. Photochem Photobiol Sci. 2010; 9:1613–20. [PubMed: 20931134]
15. Sperandio FF, Huang YY, Hamblin MR. Antimicrobial photo-dynamic therapy to kill Gram-negative bacteria. Recent Pat Antiinfect Drug Discov. 2013; 8:108–20. [PubMed: 23550545]
16. Bertoloni G, Rossi F, Valduga G, Jori G, Ali H, van Lier JE. Photosensitizing activity of water- and lipid-soluble phthalocyanines on prokaryotic and eukaryotic microbial cells. Microbios. 1992; 71:33–46. [PubMed: 1406343]
17. Maisch T, Szeimies RM, Jori G, Abels C. Antibacterial photo-dynamic therapy in dermatology. Photochem Photobiol Sci. 2004; 3:907–17. [PubMed: 15480480]
18. Resch A, Rosenstein R, Nerz C, Götz F. Differential gene expression profiling of *Staphylococcus aureus* cultivated under biofilm and planktonic conditions. Appl Environ Microbiol. 2005; 71:2663–76. [PubMed: 15870358]
19. Ehrlich GD, Arciola CR. From Koch's postulates to biofilm theory. The lesson of Bill Costerton. Int J Artif Organs. 2012; 35:695–9. [PubMed: 23138704]
20. Kashef N, Karami S, Djavid GE. Phototoxic effect of hypericin alone and in combination with acetylcysteine on *Staphylococcus aureus* biofilms. Photodiagnosis Photodyn Ther. 2015; 12:186–92. [PubMed: 25892001]
21. Demidova TN, Hamblin MR. Effect of cell-photosensitizer binding and cell density on microbial photoinactivation. Antimicrob Agents Chemother. 2005; 49:2329–35. [PubMed: 15917529]
22. Usacheva MN, Teichert MC, Biel MA. Comparison of the methylene blue and toluidine blue photobactericidal efficacy against gram-positive and gram-negative microorganisms. Lasers Surg Med. 2001; 29:165–73. [PubMed: 11553906]
23. Costerton JW, Stewart PS, Greenberg EP. Bacterial biofilms: a common cause of persistent infections. Science. 1999; 284:1318–22. [PubMed: 10334980]
24. Zanin IC, Lobo MM, Rodrigues LK, Pimenta LA, Höfling JF, Gonçalves RB. Photosensitization of in vitro biofilms by toluidine blue O combined with a light-emitting diode. Eur J Oral Sci. 2006; 114:64–9.
25. Gad F, Zahra T, Hasan T, Hamblin MR. Effects of growth phase and extracellular slime on photodynamic inactivation of gram-positive pathogenic bacteria. Antimicrob Agents Chemother. 2004; 48:2173–8. [PubMed: 15155218]
26. Wainwright M, Crossley KB. Photosensitising agents – circumventing resistance and breaking down biofilms: a review. Int Biodeterior Biodegradation. 2004; 53:119–26.
27. Kasermann F, Kempf C. Buckminsterfullerene and photodynamic inactivation of viruses. Rev Med Virol. 1998; 8:143–51. [PubMed: 10398502]

28. St Denis TG, Dai T, Izikson L, et al. All you need is light: antimicrobial photoinactivation as an evolving and emerging discovery strategy against infectious disease. Virulence. 2011; 2:509–20. [PubMed: 21971183]
29. Bliss JM, Bigelow CE, Foster TH, Haidaris CG. Susceptibility of Candida species to photodynamic effects of photofrin. Antimicrob Agents Chemother. 2004; 48:2000–6. [PubMed: 15155191]
30. Monfrecola G, Procaccini EM, Bevilacqua M, Manco A, Calabro G, Santoianni P. In vitro effect of 5-aminolaevulinic acid plus visible light on *Candida albicans*. Photochem Photobiol Sci. 2004; 3:419–22. [PubMed: 15122358]
31. Lambrechts SA, Aalders MC, Van Marle J. Mechanistic study of the photodynamic inactivation of *Candida albicans* by a cationic porphyrin. Antimicrob Agents Chemother. 2005; 49:2026–34. [PubMed: 15855528]
32. Bhawalkar JD, Kumar ND, Zhao CF, Prasad PN. Two-photon photodynamic therapy. J Clin Laser Med Surg. 1997; 15:201–4. [PubMed: 9612170]
33. Kachynski AV, Pliss A, Kuzmin AN, et al. Photodynamic therapy by in situ nonlinear photon conversion. Nature Photonics. 2014; 8:455–61.
34. Kuo WS, Chang CY, Chen HH, et al. Two-photon photoexcited photodynamic therapy and contrast agent with antimicrobial graphene quantum dots. ACS Appl Mater Interfaces. 2016; 8:30467–74. [PubMed: 27753472]
35. Attili SK, Lesar A, McNeill A, et al. An open pilot study of ambulatory photodynamic therapy using a wearable low-irradiance organic light-emitting diode light source in the treatment of nonmelanoma skin cancer. Br J Dermatol. 2009; 161:170–3. [PubMed: 19302071]
36. Mordon S, Cochrane C, Tylcz JB, Betrouni N, Mortier L, Koncar V. Light emitting fabric technologies for photodynamic therapy. Photodiagnosis Photodyn Ther. 2015; 12:1–8. [PubMed: 25481663]
37. Jarvi MT, Niedre MJ, Patterson MS, Wilson BC. The influence of oxygen depletion and photosensitizer triplet-state dynamics during photodynamic therapy on accurate singlet oxygen luminescence monitoring and analysis of treatment dose response. Photochem Photobiol. 2011; 87:223–34. [PubMed: 21143603]
38. Nielsen KP, Juzeniene A, Juzenas P, Stamnes K, Stamnes JJ, Moan J. Choice of optimal wavelength for PDT: the significance of oxygen depletion. Photochem Photobiol. 2005; 81:1190–4. [PubMed: 15934793]
39. Wiegell SR, Skiveren J, Philipsen PA, Wulf HC. Pain during photodynamic therapy is associated with protoporphyrin IX fluorescence and fluence rate. Br J Dermatol. 2008; 158:727–33. [PubMed: 18284396]
40. Jacques SL. Optical properties of biological tissues: a review. Phys Med Biol. 2013; 58:R37–61. [PubMed: 23666068]
41. van den Bergh H. On the evolution of some endoscopic light delivery systems for photodynamic therapy. Endoscopy. 1998; 30:392–407. [PubMed: 9689515]
42. Swartling J, Axelsson J, Ahlgren G, et al. System for interstitial photodynamic therapy with online dosimetry: first clinical experiences of prostate cancer. J Biomed Opt. 2010; 15:058003. [PubMed: 21054129]
43. Johansson A, Axelsson J, Andersson-Engels S, Swartling J. Realtime light dosimetry software tools for interstitial photodynamic therapy of the human prostate. Med Phys. 2007; 34:4309–21. [PubMed: 18072496]
44. Montgomery KL, Yeh AJ, Ho JS, et al. Wirelessly powered, fully internal optogenetics for brain, spinal and peripheral circuits in mice. Nat Methods. 2015; 12:969–74. [PubMed: 26280330]
45. Kim TI, McCall JG, Jung YH, et al. Injectable, cellular-scale optoelectronics with applications for wireless optogenetics. Science. 2013; 340:211–6. [PubMed: 23580530]
46. Sharma SK, Mroz P, Dai T, Huang YY, St Denis TG, Hamblin MR. Photodynamic therapy for cancer and for infections: what is the difference? Isr J Chem. 2012; 52:691–705. [PubMed: 23248387]
47. Avci P, Erdem SS, Hamblin MR. Photodynamic therapy: one step ahead with self-assembled nanoparticles. J Biomed Nano-technol. 2014; 10:1937–52.

48. Pogue BW, Samkoe KS, Gibbs-Strauss SL, Davis SC. Fluorescent molecular imaging and dosimetry tools in photodynamic therapy. Methods Mol Biol. 2010; 635:207–22. [PubMed: 20552350]
49. Pogue BW, Elliott JT, Kanick SC, et al. Revisiting photodynamic therapy dosimetry: reductionist & surrogate approaches to facilitate clinical success. Phys Med Biol. 2016; 61:R57–89. [PubMed: 26961864]
50. Dai T, Tegos GP, Zhiyentayev T, Mylonakis E, Hamblin MR. Photodynamic therapy for methicillin-resistant *Staphylococcus aureus* infection in a mouse skin abrasion model. Lasers Surg Med. 2010; 42:38–44. [PubMed: 20077489]
51. Engelhardt V, Krammer B, Plaetzer K. Antibacterial photodynamic therapy using water-soluble formulations of hypericin or mTHPC is effective in inactivation of *Staphylococcus aureus*. Photochem Photobiol Sci. 2010; 9:365–9. [PubMed: 20221463]
52. Sibani SA, McCarron PA, Woolfson AD, Donnelly RF. Photosensitiser delivery for photodynamic therapy. Part 2: systemic carrier platforms. Expert Opin Drug Deliv. 2008; 5:1241–54. [PubMed: 18976134]
53. Bombelli C, Bordi F, Ferro S, et al. New cationic liposomes as vehicles of m-tetrahydroxyphenylchlorin in photodynamic therapy of infectious diseases. Mol Pharm. 2008; 5:672–9. [PubMed: 18507469]
54. Ferro S, Ricchelli F, Mancini G, Tognon G, Jori G. Inactivation of methicillin-resistant *Staphylococcus aureus* (MRSA) by liposome-delivered photosensitising agents. J Photochem Photobiol B. 2006; 83:98–104. [PubMed: 16446097]
55. Tsai T, Yang YT, Wang TH, Chien HF, Chen CT. Improved photodynamic inactivation of gram-positive bacteria using hematoporphyrin encapsulated in liposomes and micelles. Lasers Surg Med. 2009; 41:316–22. [PubMed: 19347938]
56. Schwiertz J, Wiehe A, Gräfe S, Gitter B, Epple M. Calcium phosphate nanoparticles as efficient carriers for photodynamic therapy against cells and bacteria. Biomaterials. 2009; 30:3324–31. [PubMed: 19304318]
57. Guo Y, Rogelj S, Zhang P. Rose Bengal-decorated silica nano-particles as photosensitizers for inactivation of gram-positive bacteria. Nanotechnology. 2010; 21:065102. [PubMed: 20061596]
58. Paszko E, Ehrhardt C, Senge MO, Kelleher DP, Reynolds JV. Nan-odrug applications in photodynamic therapy. Photodiagnosis Photodyn Ther. 2011; 8:14–29. [PubMed: 21333931]
59. Yin R, Agrawal T, Khan U, et al. Antimicrobial photodynamic inactivation in nanomedicine: small light strides against bad bugs. Nanomedicine (Lond). 2015; 10:2379–404. [PubMed: 26305189]
60. Allison RR, Mota HC, Bagnato VS, Sibata CH. Bio-nanotechnology and photodynamic therapy – state of the art review. Photodiagnosis Photodyn Ther. 2008; 5:19–28. [PubMed: 19356632]
61. Sadasivam M, Avci P, Gupta GK, et al. Self-assembled liposomal nanoparticles in photodynamic therapy. Eur J Nanomed. 2013; 5doi: 10.1515/ejnm-2013-0010
62. Kozlowska D, Foran P, MacMahon P, Shelly MJ, Eustace S, O'Kennedy R. Molecular and magnetic resonance imaging: the value of immunoliposomes. Adv Drug Deliv Rev. 2009; 61:1402–11. [PubMed: 19796661]
63. Vemuri S, Rhodes CT. Preparation and characterization of liposomes as therapeutic delivery systems: a review. Pharm Acta Helv. 1995; 70:95–111. [PubMed: 7651973]
64. Jia Y, Joly H, Omri A. Characterization of the interaction between liposomal formulations and *Pseudomonas aeruginosa*. J Liposome Res. 2010; 20:134–46. [PubMed: 19831502]
65. Vilsinski BH, Gerola AP, Enumo JA, et al. Formulation of aluminum chloride phthalocyanine in pluronic(™) P-123 and F-127 block copolymer micelles: photophysical properties and photodynamic inactivation of microorganisms. Photochem Photobiol. 2015; 91:518–25. [PubMed: 25644689]
66. Couleaud P, Morosini V, Frochot C, Richeter S, Raehm L, Durand JO. Silica-based nanoparticles for photodynamic therapy applications. Nanoscale. 2010; 2:1083–95. [PubMed: 20648332]
67. Huang YY, Sharma SK, Dai T, et al. Can nanotechnology potentiate photodynamic therapy? Nanotechnol Rev. 2012; 1:111–46. [PubMed: 26361572]

68. Perni S, Prokopovich P, Pratten J, Parkin IP, Wilson M. Nanoparticles: their potential use in antibacterial photodynamic therapy. Photochem Photobiol Sci. 2011; 10:712–20. [PubMed: 21380441]
69. Chen RJ, Chen PC, Prasannan A, et al. Formation of gold decorated porphyrin nanoparticles and evaluation of their photo-thermal and photodynamic activity. Mater Sci Eng C Mater Biol Appl. 2016; 63:678–85. [PubMed: 27040265]
70. Chu CK, Tu YC, Hsiao JH, et al. Combination of photothermal and photodynamic inactivation of cancer cells through surface plasmon resonance of a gold nanoring. Nanotechnology. 2016; 27:115102. [PubMed: 26878331]
71. Cheng Y, Meyers JD, Broome AM, Kenney ME, Basilion JP, Burda C. Deep penetration of a PDT drug into tumors by noncovalent drug-gold nanoparticle conjugates. J Am Chem Soc. 2011; 133:2583–91. [PubMed: 21294543]
72. Hu Y, Yang Y, Wang H, Du H. Synergistic integration of layer-by-layer assembly of photosensitizer and gold nanorings for enhanced photodynamic therapy in the near infrared. ACS Nano. 2015; 9:8744–54. [PubMed: 26267273]
73. Wang X, Yang L, Chen ZG, Shin DM. Application of nanotechnology in cancer therapy and imaging. CA Cancer J Clin. 2008; 58:97–110. [PubMed: 18227410]
74. Sherwani MA, Tufail S, Khan AA, Owais M. Gold nanoparticle-photosensitizer conjugate based photodynamic inactivation of biofilm producing cells: potential for treatment of *C albicans* infection in BALB/c mice. PLoS One. 2015; 10:e0131684. [PubMed: 26148012]
75. Tawfik AA, Alsharnoubi J, Morsy M. Photodynamic antibacterial enhanced effect of methylene blue-gold nanoparticles conjugate on *Staphylococcal aureus* isolated from impetigo lesions in vitro study. Photodiagnosis Photodyn Ther. 2015; 12:215–20. [PubMed: 25827622]
76. Khan S, Alam F, Azam A, Khan AU. Gold nanoparticles enhance methylene blue-induced photodynamic therapy: a novel therapeutic approach to inhibit *Candida albicans* biofilm. Int J Nanomedicine. 2012; 7:3245–57. [PubMed: 22802686]
77. Dakal TC, Kumar A, Majumdar RS, Yadav V. Mechanistic basis of antimicrobial actions of silver nanoparticles. Front Microbiol. 2016; 7:1831. [PubMed: 27899918]
78. Duran N, Durán M, de Jesus MB, Seabra AB, Fávaro WJ, Nakazato G. Silver nanoparticles: a new view on mechanistic aspects on antimicrobial activity. Nanomedicine. 2016; 12:789–99. [PubMed: 26724539]
79. Gupta A, Silver S. Silver as a biocide: will resistance become a problem? Nat Biotechnol. 1998; 16:888. [PubMed: 9788326]
80. Matsumura Y, Yoshikata K, Kunisaki S, Tsuchido T. Mode of bactericidal action of silver zeolite and its comparison with that of silver nitrate. Appl Environ Microbiol. 2003; 69:4278–81. [PubMed: 12839814]
81. Smetana AB, Klabunde KJ, Marchin GR, Sorensen CM. Biocidal activity of nanocrystalline silver powders and particles. Langmuir. 2008; 24:7457–64. [PubMed: 18543995]
82. Holt KB, Bard AJ. Interaction of silver(I) ions with the respiratory chain of *Escherichia coli*: an electrochemical and scanning electrochemical microscopy study of the antimicrobial mechanism of micromolar Ag^+ Biochemistry. 2005; 44:13214–23. [PubMed: 16185089]
83. Dibrov P, Dzioba J, Gosink KK, Häse CC. Chemiosmotic mechanism of antimicrobial activity of Ag(+) in *Vibrio cholerae*. Antimicrob Agents Chemother. 2002; 46:2668–70. [PubMed: 12121953]
84. Sondi I, Salopek-Sondi B. Silver nanoparticles as antimicrobial agent: a case study on *E coli* as a model for Gram-negative bacteria. J Colloid Interface Sci. 2004; 275:177–82. [PubMed: 15158396]
85. Panacek A, Kvítek L, Prucek R, et al. Silver colloid nanoparticles: synthesis, characterization, and their antibacterial activity. J Phys Chem B. 2006; 110:16248–53. [PubMed: 16913750]
86. Zhang XF, Liu ZG, Shen W, et al. Silver nanoparticles: synthesis, characterization, properties, applications, and therapeutic approaches. Int J Mol Sci. 2016; 17 pii: E1534. doi: 10.3390/ijms17091534
87. Martinez-Castanon GA, Niño-Martínez N, Martínez-Gutierrez F, Martínez-Mendoza JR, Ruiz F. Synthesis and antibacterial activity of silver nanoparticles with different sizes. J Nanopart Res. 2008; 10:1343–8.

88. Pal S, Tak YK, Song JM. Does the antibacterial activity of silver nanoparticles depend on the shape of the nanoparticle? A study of the Gram-negative bacterium *Escherichia coli*. Appl Environ Microbiol. 2007; 73:1712–20. [PubMed: 17261510]
89. Brett DW. A discussion of silver as an antimicrobial agent: alleviating the confusion. Ostomy Wound Manage. 2006; 52:34–41.
90. Dhawan A, Sharma V. Toxicity assessment of nanomaterials: methods and challenges. Anal Bioanal Chem. 2010; 398:589–605. [PubMed: 20652549]
91. McGillicuddy E, Murray I, Kavanagh S, et al. Silver nanoparticles in the environment: sources, detection and ecotoxicology. Sci Total Environ. 2017; 575:231–46. [PubMed: 27744152]
92. Sigg L, Behra R, Groh K, et al. Chemical aspects of nanoparticle ecotoxicology. Chimia (Aarau). 2014; 68:806–11. [PubMed: 26508489]
93. Hoheisel SM, Diamond S, Mount D. Comparison of nanosilver and ionic silver toxicity in *Daphnia magna* and *Pimephales promelas*. Environ Toxicol Chem. 2012; 31:2557–63. [PubMed: 22887018]
94. Lubick N. Nanosilver toxicity: ions, nanoparticles – or both? Environ Sci Technol. 2008; 42:8617. [PubMed: 19192768]
95. Navarro E, Piccapietra F, Wagner B, et al. Toxicity of silver nanoparticles to *Chlamydomonas reinhardtii*. Environ Sci Technol. 2008; 42:8959–64. [PubMed: 19192825]
96. Ivask A, Kurvet I, Kasemets K, et al. Size-dependent toxicity of silver nanoparticles to bacteria, yeast, algae, crustaceans and mammalian cells in vitro. PLoS One. 2014; 9:e102108. [PubMed: 25048192]
97. Velusamy P, Kumar GV, Jeyanthi V, Das J, Pachaiappan R. Bio-inspired green nanoparticles: synthesis, mechanism, and antibacterial application. Toxicol Res. 2016; 32:95–102. [PubMed: 27123159]
98. Klaus T, Joerger R, Olsson E, Granqvist CG. Silver-based crystalline nanoparticles, microbially fabricated. Proc Natl Acad Sci USA. 1999; 96:13611–4. [PubMed: 10570120]
99. Samadi N, Golkaran D, Eslamifar A, Jamalifar H, Fazeli MR, Mohseni FA. Intra/extracellular biosynthesis of silver nanoparticles by an autochthonous strain of *Proteus mirabilis* isolated from photographic waste. J Biomed Nanotechnol. 2009; 5:247–53. [PubMed: 20055006]
100. Gurunathan S, Kalishwaralal K, Vaidyanathan R, et al. Biosynthesis, purification and characterization of silver nanoparticles using *Escherichia coli*. Colloids Surf B Biointerfaces. 2009; 74:328–35. [PubMed: 19716685]
101. Vigneshwaran N, Kathe AA, Varadarajan PV, Nachane RP, Balasubramanya RH. Biomimetics of silver nanoparticles by white rot fungus, *Phaenerochaete chrysosporium*. Colloids Surf B Biointerfaces. 2006; 53:55–9. [PubMed: 16962745]
102. Morsy FM. Toward revealing the controversy of bacterial biosynthesis versus bactericidal properties of silver nanoparticles (AgNPs): bacteria and other microorganisms do not per se viably synthesize AgNPs. Arch Microbiol. 2015; 197:645–55. [PubMed: 25724923]
103. Pollini M, Russo M, Licciulli A, Sannino A, Maffezzoli A. Characterization of antibacterial silver coated yarns. J Mater Sci Mater Med. 2009; 20:2361–6. [PubMed: 19526328]
104. Holtz RD, Lima BA, Souza Filho AG, Brocchi M, Alves OL. Nanostructured silver vanadate as a promising antibacterial additive to water-based paints. Nanomedicine. 2012; 8:935–40.
105. Abdullayev E, Sakakibara K, Okamoto K, Wei W, Ariga K, Lvov Y. Natural tubule clay template synthesis of silver nanorods for antibacterial composite coating. ACS Appl Mater Interfaces. 2011; 3:4040–6. [PubMed: 21905653]
106. Kumar A, Vemula PK, Ajayan PM, John G. Silver-nanoparticle-embedded antimicrobial paints based on vegetable oil. Nat Mater. 2008; 7:236–41. [PubMed: 18204453]
107. Misba L, Kulshrestha S, Khan AU. Antibiofilm action of a toluidine blue O-silver nanoparticle conjugate on *Streptococcus mutans*: a mechanism of type I photodynamic therapy. Biofouling. 2016; 32:313–28. [PubMed: 26905507]
108. Sharma SK, Chiang LY, Hamblin MR. Photodynamic therapy with fullerenes in vivo: reality or a dream? Nanomedicine (UK). 2011; 6:1813–25.
109. Mroz P, Tegos GP, Gali H, Wharton T, Sarna T, Hamblin MR. Photodynamic therapy with fullerenes. Photochem Photobiol Sci. 2007; 6:1139–49. [PubMed: 17973044]

110. Huang L, Terakawa M, Zhiyentayev T, et al. Innovative cationic fullerenes as broad-spectrum light-activated antimicrobials. Nanomedicine. 2010; 6:442–52. [PubMed: 19914400]
111. Lu Z, Dai T, Huang L, et al. Photodynamic therapy with a cationic functionalized fullerene rescues mice from fatal wound infections. Nanomedicine (UK). 2010; 5:1525–33.
112. Mizuno K, Zhiyentayev T, Huang L, et al. Antimicrobial photodynamic therapy with functionalized fullerenes: quantitative structure-activity relationships. J Nanomed Nanotechnol. 2011; 2:109–17.
113. Thota S, Wang M, Jeon S, Maragani S, Hamblin MR, Chiang LY. Synthesis and characterization of positively charged pentacationic [60]fullerene monoadducts for antimicrobial photodynamic inactivation. Molecules. 2012; 17:5225–43. [PubMed: 22565476]
114. Zhang Y, Dai T, Wang M, Vecchio D, Chiang LY, Hamblin MR. Potentiation of antimicrobial photodynamic inactivation mediated by a cationic fullerene by added iodide: in vitro and in vivo studies. Nanomedicine (Lond). 2015; 10:603–14. [PubMed: 25723093]
115. Caputo F, De Nicola M, Ghibelli L. Pharmacological potential of bioactive engineered nanomaterials. Biochem Pharmacol. 2014; 92:112–30. [PubMed: 25175739]
116. Anilkumar P, Lu F, Cao L, et al. Fullerenes for applications in biology and medicine. Curr Med Chem. 2011; 18:2045–59. [PubMed: 21517770]
117. Huang Y, Sharma SK, Yin R, Agrawal T, Chiang LY, Hamblin MR. Functionalized fullerenes in photodynamic therapy. J Biomed Nanotechnol. 2014; 10:1918–36. [PubMed: 25544837]
118. Jeon S, Haley J, Flikkema J, et al. Linear and nonlinear optical properties of photoresponsive [60]fullerene hybrid triads and tetrads with dual NIR two-photon absorption characteristics. J Phys Chem C Nanomater Interfaces. 2013; 117:17186–95. [PubMed: 24163713]
119. Jeon S, Wang M, Tan LS, Cooper T, Hamblin MR, Chiang LY. Synthesis of photoresponsive dual NIR two-photon absorptive [60]fullerene triads and tetrads. Molecules. 2013; 18:9603–22. [PubMed: 23941881]
120. Tegos GP, Demidova TN, Arcila-Lopez D, et al. Cationic fullerenes are effective and selective antimicrobial photosensitizers. Chem Biol. 2005; 12:1127–35. [PubMed: 16242655]
121. Wang M, Maragani S, Huang L, et al. Synthesis of decacationic [60]fullerene decaiodides giving photoinduced production of superoxide radicals and effective PDT-mediation on antimicrobial photoinactivation. Eur J Med Chem. 2013; 63C:170–84.
122. Wang M, Huang L, Sharma SK, et al. Synthesis and photodynamic effect of new highly photostable decacationically armed [60]-and [70]fullerene decaiodide monoadducts to target pathogenic bacteria and cancer cells. J Med Chem. 2012; 55:4274–85. [PubMed: 22512669]
123. Aoshima H, Kokubo K, Shirakawa S, Ito M, Yamana S, Oshima T. Antimicrobial activity of fullerenes and their hydroxylated derivatives. Biocontrol Sci. 2009; 14:69–72. [PubMed: 19579658]
124. Huang L, Wang M, Sharma SK, et al. Decacationic [70] fullerene approach for efficient photokilling of infectious bacteria and cancer cells. ECS Trans. 2013; 45doi: 10.1149/04520.0065ecst
125. Milanesio ME, Spesia MB, Cormick MP, Durantini EN. Mechanistic studies on the photodynamic effect induced by a dicationic fullerene C60 derivative on *Escherichia coli* and *Candida albicans* cells. Photodiagnosis Photodyn Ther. 2013; 10:320–7. [PubMed: 23993859]
126. Mohr H, Knüver-Hopf J, Gravemann U, Redecker-Klein A, Müller TH. West Nile virus in plasma is highly sensitive to methylene blue-light treatment. Transfusion. 2004; 44:886–90. [PubMed: 15157256]
127. Kasermann F, Kempf C. Photodynamic inactivation of enveloped viruses by buckminsterfullerene. Antiviral Res. 1997; 34:65–70. [PubMed: 9107386]
128. Lipovsky A, Gedanken A, Nitzan Y, Lubart R. Enhanced inactivation of bacteria by metal-oxide nanoparticles combined with visible light irradiation. Lasers Surg Med. 2011; 43:236–40. [PubMed: 21412807]
129. Konaka R, Kasahara E, Dunlap WC, Yamamoto Y, Chien KC, Inoue M. Irradiation of titanium dioxide generates both singlet oxygen and superoxide anion. Free Radic Biol Med. 1999; 27:294–300. [PubMed: 10468201]

130. Konaka R, Kasahara E, Dunlap WC, Yamamoto Y, Chien KC, Inoue M. Ultraviolet irradiation of titanium dioxide in aqueous dispersion generates singlet oxygen. Redox Rep. 2001; 6:319–25. [PubMed: 11778850]

131. Wu TS, Wang KX, Li GD, Sun SY, Sun J, Chen JS. Montmorillonite-supported Ag/TiO(2) nanoparticles: an efficient visible-light bacteria photodegradation material. ACS Appl Mater Interfaces. 2010; 2:544–50. [PubMed: 20356203]

132. Leyland NS, Podporska-Carroll J, Browne J, Hinder SJ, Quilty B, Pillai SC. Highly efficient F, Cu doped TiO_2 anti-bacterial visible light active photocatalytic coatings to combat hospital-acquired infections. Sci Rep. 2016; 6:24770. [PubMed: 27098010]

133. Foster HA, Ditta IB, Varghese S, Steele A. Photocatalytic disinfection using titanium dioxide: spectrum and mechanism of antimicrobial activity. Appl Microbiol Biotechnol. 2011; 90:1847–68. [PubMed: 21523480]

134. Mills A, Le Hunte S. An overview of semiconductor photocatalysis. J Photochem Photobiol A. 1997; 108:1–35.

135. Byrne JA, Dunlop PS, Hamilton JW, et al. A review of heterogeneous photocatalysis for water and surface disinfection. Molecules. 2015; 20:5574–615. [PubMed: 25830789]

136. Li Puma G, Rodriguez-Gonzalez V, Perez-Larios A. Photocatalysis: from the treatment of emerging contaminants to energy conversion. J Hazard Mater. 2013; 263(Pt 1):1. [PubMed: 24267571]

137. Oliveira HG, Ferreira LH, Bertazzoli R, Longo C. Remediation of 17-alpha-ethinylestradiol aqueous solution by photocatalysis and electrochemically-assisted photocatalysis using TiO_2 and TiO_2/WO_3 electrodes irradiated by a solar simulator. Water Res. 2015; 72:305–14. [PubMed: 25238917]

138. Saggioro EM, Oliveira AS, Pavesi T, Maia CG, Ferreira LF, Moreira JC. Use of titanium dioxide photocatalysis on the remediation of model textile wastewaters containing azo dyes. Molecules. 2011; 16:10370–86. [PubMed: 22169940]

139. Kim S, Ghafoor K, Lee J, et al. Bacterial inactivation in water, DNA strand breaking, and membrane damage induced by ultraviolet-assisted titanium dioxide photocatalysis. Water Res. 2013; 47:4403–11. [PubMed: 23764591]

140. Rizzo L, Della Sala A, Fiorentino A, Li Puma G. Disinfection of urban wastewater by solar driven and UV lamp – TiO(2) photocatalysis: effect on a multi drug resistant *Escherichia coli* strain. Water Res. 2014; 53:145–52. [PubMed: 24525064]

141. Robertson PK, Robertson JM, Bahnemann DW. Removal of microorganisms and their chemical metabolites from water using semiconductor photocatalysis. J Hazard Mater. 2012:211–212. 161–71. [PubMed: 22633883]

142. Yamada N, Suzumura M, Koiwa F, Negishi N. Differences in elimination efficiencies of *Escherichia coli* in freshwater and seawater as a result of TiO_2 photocatalysis. Water Res. 2013; 47:2770–6. [PubMed: 23523173]

143. Vidal A. Developments in solar photocatalysis for water purification. Chemosphere. 1998; 36:2593–606. [PubMed: 9570109]

144. Sekiguchi Y, Yao Y, Ohko Y, et al. Self-sterilizing catheters with titanium dioxide photocatalyst thin films for clean intermittent catheterization: basis and study of clinical use. Int J Urol. 2007; 14:426–30. [PubMed: 17511726]

145. Nakamura H, Tanaka M, Shinohara S, Gotoh M, Karube I. Development of a self-sterilizing lancet coated with a titanium dioxide photocatalytic nano-layer for self-monitoring of blood glucose. Biosens Bioelectron. 2007; 22:1920–5. [PubMed: 16987650]

146. Chawengkijwanich C, Hayata Y. Development of TiO_2 powder-coated food packaging film and its ability to inactivate *Escherichia coli* in vitro and in actual tests. Int J Food Microbiol. 2008; 123:288–92. [PubMed: 18262298]

147. Suketa N, Sawase T, Kitaura H, et al. An antibacterial surface on dental implants, based on the photocatalytic bactericidal effect. Clin Implant Dent Relat Res. 2005; 7:105–11. [PubMed: 15996357]

148. Lilja M, Forsgren J, Welch K, Astrand M, Engqvist H, Strømme M. Photocatalytic and antimicrobial properties of surgical implant coatings of titanium dioxide deposited though cathodic arc evaporation. Biotechnol Lett. 2012; 34:2299–305. [PubMed: 22941372]

149. Mitoraj D, Jańczyk A, Strus M, et al. Visible light inactivation of bacteria and fungi by modified titanium dioxide. Photochem Photobiol Sci. 2007; 6:642–8. [PubMed: 17549266]

150. Wong CL, Tan YN, Mohamed AR. A review on the formation of titania nanotube photocatalysts by hydrothermal treatment. J Environ Manage. 2011; 92:1669–80. [PubMed: 21450395]

151. Ohtani B, Prieto-Mahaney OO, Li D, Abe R. What is Degussa (Evonik) P25? Crystalline composition analysis, reconstruction from isolated pure particles and photocatalytic activity test. J Photochem Photobiol A: Chem. 2010; 216:179–182.

152. Juzenas P, Chen W, Sun YP, et al. Quantum dots and nanoparticles for photodynamic and radiation therapies of cancer. Adv Drug Deliv Rev. 2008; 60:1600–14. [PubMed: 18840487]

153. Bakalova R, Ohba H, Zhelev Z, Ishikawa M, Baba Y. Quantum dots as photosensitizers? Nat Biotechnol. 2004; 22:1360–1. [PubMed: 15529155]

154. Yaghini E, Seifalian AM, MacRobert AJ. Quantum dots and their potential biomedical applications in photosensitization for photodynamic therapy. Nanomedicine (Lond). 2009; 4:353–63. [PubMed: 19331542]

155. Narband N, Mubarak M, Ready D, et al. Quantum dots as enhancers of the efficacy of bacterial lethal photosensitization. Nanotechnology. 2008; 19:445102. [PubMed: 21832719]

156. Chen G, Qiu H, Prasad PN, Chen X. Upconversion nanoparticles: design, nanochemistry, and applications in theranostics. Chem Rev. 2014; 114:5161–214. [PubMed: 24605868]

157. Prasad, PN. Introduction to nanomedicine and nanobioengineering. Hoboken, NJ: Wiley-Interscience; 2012.

158. Prasad, PN. Introduction to biophotonics. Hoboken, NJ: Wiley-Interscience; 2003.

159. Wainwright M. Local treatment of viral disease using photodynamic therapy. Int J Antimicrob Agents. 2003; 21:510–20. [PubMed: 12791463]

160. Lim ME, Lee YL, Zhang Y, Chu JJ. Photodynamic inactivation of viruses using upconversion nanoparticles. Biomaterials. 2012; 33:1912–20. [PubMed: 22153019]

161. Larraneta E, McCrudden MT, Courtenay AJ, Donnelly RF. Microneedles: a new frontier in nanomedicine delivery. Pharm Res. 2016; 33:1055–73. [PubMed: 26908048]

162. Kolli CS. Microneedles: bench to bedside. Ther Deliv. 2015; 6:1081–8. [PubMed: 26419290]

163. Kearney MC, Brown S, McCrudden MT, Brady AJ, Donnelly RF. Potential of microneedles in enhancing delivery of photosensitising agents for photodynamic therapy. Photodiagnosis Photodyn Ther. 2014; 11:459–66. [PubMed: 25291556]

164. Caffarel-Salvador E, Kearney MC, et al. Methylene blue-loaded dissolving microneedles: potential use in photodynamic antimicrobial chemotherapy of infected wounds. Pharmaceutics. 2015; 7:397–412. [PubMed: 26426040]

165. Poole K. Efflux-mediated antimicrobial resistance. J Antimicrob Chemother. 2005; 56:20–51. [PubMed: 15914491]

166. Wainwright M, Crossley KB. Methylene blue – a therapeutic dye for all seasons? J Chemother. 2002; 14:431–43. [PubMed: 12462423]

167. Bhatti M, MacRobert A, Meghji S, Henderson B, Wilson M. A study of the uptake of toluidine blue O by *Porphyromonas gingivalis* and the mechanism of lethal photosensitization. Photochem Photobiol. 1998; 68:370–6. [PubMed: 9747591]

168. O'Neill J, Wilson M, Wainwright M. Comparative antistreptococcal activity of photobactericidal agents. J Chemother. 2003; 15:329–34. [PubMed: 12962360]

169. Phoenix DA, Sayed Z, Hussain S, Harris F, Wainwright M. The phototoxicity of phenothiazinium derivatives against *Escherichia coli* and *Staphylococcus aureus*. FEMS Immunol Med Microbiol. 2003; 39:17–22. [PubMed: 14556991]

170. Romanova NA, Brovko LY, Moore L, et al. Assessment of photodynamic destruction of *Escherichia coli* O157:H7 and *Listeria monocytogenes* by using ATP bioluminescence. Appl Environ Microbiol. 2003; 69:6393–8. [PubMed: 14602591]

171. Wong TW, Wang YY, Sheu HM, Chuang YC. Bactericidal effects of toluidine blue-mediated photodynamic action on *Vibrio vulnificus*. Antimicrob Agents Chemother. 2005; 49:895–902. [PubMed: 15728881]

172. Huang L, Xuan Y, Koide Y, Zhiyentayev T, Tanaka M, Hamblin MR. Type I and type II mechanisms of antimicrobial photodynamic therapy: an in vitro study on gram-negative and gram-positive bacteria. Lasers Surg Med. 2012; 44:490–9. [PubMed: 22760848]

173. de Oliveira BP, Aguiar CM, Camara AC. Photodynamic therapy in combating the causative microorganisms from endodontic infections. Eur J Dent. 2014; 8:424–30. [PubMed: 25202228]

174. Klepac-Ceraj V, Patel N, Song X, et al. Photodynamic effects of methylene blue-loaded polymeric nanoparticles on dental plaque bacteria. Lasers Surg Med. 2011; 43:600–6. [PubMed: 22057487]

175. Siddiqui SH, Awan KH, Javed F. Bactericidal efficacy of photodynamic therapy against *Enterococcus faecalis* in infected root canals: a systematic literature review. Photodiagnosis Photodyn Ther. 2013; 10:632–43. [PubMed: 24192536]

176. Wainwright M, Phoenix DA, Laycock SL, Wareing DR, Wright PA. Photobactericidal activity of phenothiazinium dyes against methicillin-resistant strains of *Staphylococcus aureus*. FEMS Microbiol Lett. 1998; 160:177–81. [PubMed: 9532735]

177. Tegos GP, Hamblin MR. Phenothiazinium antimicrobial photosensitizers are substrates of bacterial multidrug resistance pumps. Antimicrob Agents Chemother. 2006; 50:196–203. [PubMed: 16377686]

178. Tegos GP, Masago K, Aziz F, Higginbotham A, Stermitz FR, Hamblin MR. Inhibitors of bacterial multidrug efflux pumps potentiate antimicrobial photoinactivation. Antimicrob Agents Chemother. 2008; 52:3202–9. [PubMed: 18474586]

179. Kishen A, Upadya M, Tegos GP, Hamblin MR. Efflux pump inhibitor potentiates antimicrobial photodynamic inactivation of *Enterococcus faecalis* biofilm. Photochem Photobiol. 2010; 86:1343–9. [PubMed: 20860692]

180. Prates RA, Kato IT, Ribeiro MS, Tegos GP, Hamblin MR. Influence of multidrug efflux systems on methylene blue-mediated photodynamic inactivation of *Candida albicans*. J Antimicrob Chemother. 2011; 66:1525–32. [PubMed: 21525022]

181. Huang L, St Denis TG, Xuan Y, et al. Paradoxical potentiation of methylene blue-mediated antimicrobial photodynamic inactivation by sodium azide: role of ambient oxygen and azide radicals. Free Radic Biol Med. 2012; 53:2062–71. [PubMed: 23044264]

182. Li MY, Cline CS, Koker EB, Carmichael HH, Chignell CF, Bilski P. Quenching of singlet molecular oxygen (102) by azide anion in solvent mixtures. Photochem Photobiol. 2001; 74:760–4. [PubMed: 11783930]

183. Tavares A, Dias SR, Carvalho CM, et al. Mechanisms of photodynamic inactivation of a gram-negative recombinant bioluminescent bacterium by cationic porphyrins. Photochem Photobiol Sci. 2011; 10:1659–69. [PubMed: 21799996]

184. Kasimova KR, Sadasivam M, Landi G, Sarna T, Hamblin MR. Potentiation of photoinactivation of Gram-positive and Gram-negative bacteria mediated by six phenothiazinium dyes by addition of azide ion. Photochem Photobiol Sci. 2014; 13:1541–8. [PubMed: 25177833]

185. Lichstein HC, Soule MH. Studies of the effect of sodium azide on microbic growth and respiration: I. The action of sodium azide on microbic growth. J Bacteriol. 1944; 47:221–30. [PubMed: 16560767]

186. Yin R, Wang M, Huang YY, et al. Antimicrobial photodynamic inactivation with decacationic functionalized fullerenes: oxygen independent photokilling in presence of azide and new mechanistic insights. Free Radic Biol Med. 2015; 79:14–27. [PubMed: 25451642]

187. Malešič J, Strlič M, Kolar J, Polanc S. The influence of halide and pseudo-halide antioxidants in Fenton-like reaction systems containing copper(II) ions. J Mol Catal A Chem. 2005; 241:126–32.

188. St Denis TG, Vecchio D, Zadlo A, et al. Thiocyanate potentiates antimicrobial photodynamic therapy: in situ generation of the sulfur trioxide radical anion by singlet oxygen. Free Radic Biol Med. 2013; 65C:800–10.

189. Vecchio D, Gupta A, Huang L, et al. Bacterial photodynamic inactivation mediated by methylene blue and red light is enhanced by synergistic effect of potassium iodide. Antimicrob Agents Chemother. 2015; 59:5203–12. [PubMed: 26077247]

190. Administration FDA. Guidance on potassium iodide as a thyroid blocking agent in radiation emergencies. Washington, DC: Food and Drug Administration; 2001.
191. Xue SL, Li L. Oral potassium iodide for the treatment of sporotrichosis. Mycopathologia. 2009; 167:355–6. [PubMed: 19130293]
192. Huang YY, Choi H, Kushida Y, Bhayana B, Wang Y, Hamblin MR. Broad-spectrum antimicrobial effects of photocatalysis using titanium dioxide nanoparticles are strongly potentiated by addition of potassium iodide. Antimicrob Agents Chemother. 2016; 60:5445–53. [PubMed: 27381399]
193. Freire F, Ferraresi C, Jorge AO, Hamblin MR. Photodynamic therapy of oral Candida infection in a mouse model. J Photochem Photobiol B. 2016; 159:161–8. [PubMed: 27074245]
194. Wu X, Huang YY, Kushida Y, Bhayana B, Hamblin MR. Broad-spectrum antimicrobial photocatalysis mediated by titanium dioxide and UVA is potentiated by addition of bromide ion via formation of hypobromite. Free Radic Biol Med. 2016; 95:74–81. [PubMed: 27012419]
195. Dai T, Huang YY, Hamblin MR. Photodynamic therapy for localized infections – state of the art. Photodiagnosis Photodyn Ther. 2009; 6:170–88. [PubMed: 19932449]
196. Demidova TN, Gad F, Zahra T, Francis KP, Hamblin MR. Monitoring photodynamic therapy of localized infections by bioluminescence imaging of genetically engineered bacteria. J Photochem Photobiol B. 2005; 81:15–25. [PubMed: 16040251]
197. Gad F, Zahra T, Francis KP, Hasan T, Hamblin MR. Targeted photodynamic therapy of established soft-tissue infections in mice. Photochem Photobiol Sci. 2004; 3:451–8. [PubMed: 15122362]
198. Hamblin MR, O'Donnell DA, Murthy N, Contag CH, Hasan T. Rapid control of wound infections by targeted photodynamic therapy monitored by in vivo bioluminescence imaging. Photochem Photobiol. 2002; 75:51–7. [PubMed: 11837327]
199. Hamblin MR, Zahra T, Contag CH, McManus AT, Hasan T. Optical monitoring and treatment of potentially lethal wound infections in vivo. J Infect Dis. 2003; 187:1717–26. [PubMed: 12751029]
200. Tawfik AA, Noaman I, El-Elsayyad H, El-Mashad N, Soliman M. A study of the treatment of cutaneous fungal infection in animal model using photoactivated composite of methylene blue and gold nanoparticle. Photodiagnosis Photodyn Ther. 2016; 15:59–69. [PubMed: 27242275]
201. Huang L, Wang M, Dai T, et al. Antimicrobial photodynamic therapy with decacationic monoadducts and bisadducts of [70]fullerene: in vitro and in vivo studies. Nanomedicine (Lond). 2014; 9:253–66. [PubMed: 23738632]
202. Grinholc M, Nakonieczna J, Fila G, et al. Antimicrobial photodynamic therapy with fulleropyrrolidine: photoinactivation mechanism of *Staphylococcus aureus*, in vitro and in vivo studies. Appl Microbiol Biotechnol. 2015; 99:4031–43. [PubMed: 25820601]
203. Nafee N, Youssef A, El-Gowelli H, Asem H, Kandil S. Antibiotic-free nanotherapeutics: hypericin nanoparticles thereof for improved in vitro and in vivo antimicrobial photodynamic therapy and wound healing. Int J Pharm. 2013; 454:249–58. [PubMed: 23834835]
204. Buchholz J, Walt H. Veterinary photodynamic therapy: a review. Photodiagnosis Photodyn Ther. 2013; 10:342–7. [PubMed: 24284083]
205. Hawkins JA, Johnson-Delivorias MH, Heitz JR. Photodynamic action of erythrosin B as a toxic mechanism for infective larvae of bovine gastrointestinal nematodes. Vet Parasitol. 1986; 21:265–70. [PubMed: 3022460]
206. Silva LA, Novaes AB Jr, de Oliveira RR, Nelson-Filho P, Santam-aria M Jr, Silva RA. Antimicrobial photodynamic therapy for the treatment of teeth with apical periodontitis: a histopathological evaluation. J Endod. 2012; 38:360–6. [PubMed: 22341075]
207. de Oliveira RR, Novaes AB Jr, Garlet GP, et al. The effect of a single episode of antimicrobial photodynamic therapy in the treatment of experimental periodontitis. Microbiological profile and cytokine pattern in the dog mandible. Lasers Med Sci. 2011; 26:359–67. [PubMed: 21086009]
208. Sellera FP, Sabino CP, Ribeiro MS, et al. In vitro photoinactivation of bovine mastitis related pathogens. Photodiagnosis Photodyn Ther. 2016; 13:276–81. [PubMed: 26315923]
209. Hayek RR, Araújo NS, Gioso MA, et al. Comparative study between the effects of photodynamic therapy and conven tional therapy on microbial reduction in ligature-induced peri-implantitis in dogs. J Periodontol. 2005; 76:1275–81. [PubMed: 16101358]

210. Nascimento CL, Ribeiro MS, Sellera FP, Dutra GH, Simões A, Teixeira CR. Comparative study between photodynamic and antibiotic therapies for treatment of footpad dermatitis (bumblefoot) in Magellanic penguins (*Spheniscus magellanicus*). Photodiagnosis Photodyn Ther. 2015; 12:36–44. [PubMed: 25573284]
211. Sellera FP, Sabino CP, Ribeiro MS, et al. Photodynamic therapy for pododermatitis in penguins. Zoo Biol. 2014; 33:353–6. [PubMed: 24888264]
212. Kharkwal GB, Sharma SK, Huang YY, Dai T, Hamblin MR. Photodynamic therapy for infections: clinical applications. Lasers Surg Med. 2011; 43:755–67. [PubMed: 22057503]
213. Morley S, Griffiths J, Philips G, et al. Phase IIa randomized, placebo-controlled study of antimicrobial photodynamic therapy in bacterially colonized, chronic leg ulcers and diabetic foot ulcers: a new approach to antimicrobial therapy. Br J Dermatol. 2013; 168:617–24. [PubMed: 23066973]
214. Asilian A, Davami M. Comparison between the efficacy of photodynamic therapy and topical paromomycin in the treatment of Old World cutaneous leishmaniasis: a placebo-controlled, randomized clinical trial. Clin Exp Dermatol. 2006; 31:634–7. [PubMed: 16780497]
215. Abduljabbar T. Effect of mechanical debridement with adjunct antimicrobial photodynamic therapy in the treatment of periimplant diseases in type-2 diabetic smokers and non-smokers. Photodiagnosis Photodyn Ther. 2017; 17:111–4. [PubMed: 27884740]
216. Pavlič A, Matoh U, Rajić V, Petelin M. Effect of repeated antimicrobial photodynamic therapy in treatment of periodontitis associated with Fanconi anemia. Photomed Laser Surg. 2017; 35:64–8. [PubMed: 27626108]
217. Panhoca VH, Esteban Florez FL, Corrêa TQ, Paolillo FR, de Souza CW, Bagnato VS. Oral decontamination of orthodontic patients using photodynamic therapy mediated by blue-light irradiation and curcumin associated with sodium dodecyl sulfate. Photomed Laser Surg. 2016; 34:411–7. [PubMed: 27454528]
218. de Freitas LM, Calixto GM, Chorilli M, et al. Polymeric nanoparticle-based photodynamic therapy for chronic periodontitis in vivo. Int J Mol Sci. 2016; 17 pii: E769. doi: 10.3390/ijms17050769
219. Chan VS. Nanomedicine: an unresolved regulatory issue. Regul Toxicol Pharmacol. 2006; 46:218–24. [PubMed: 17081666]
220. Ferrari M. Cancer nanotechnology: opportunities and challenges. Nat Rev Cancer. 2005; 5:161–71. [PubMed: 15738981]
221. Vega-Villa KR, Takemoto JK, Yáñez JA, Remsberg CM, Forrest ML, Davies NM. Clinical toxicities of nanocarrier systems. Adv Drug Deliv Rev. 2008; 60:929–38. [PubMed: 18313790]
222. Warheit DB. Nanoparticles: health impacts? Mater Today. 2004; 7:32–5.

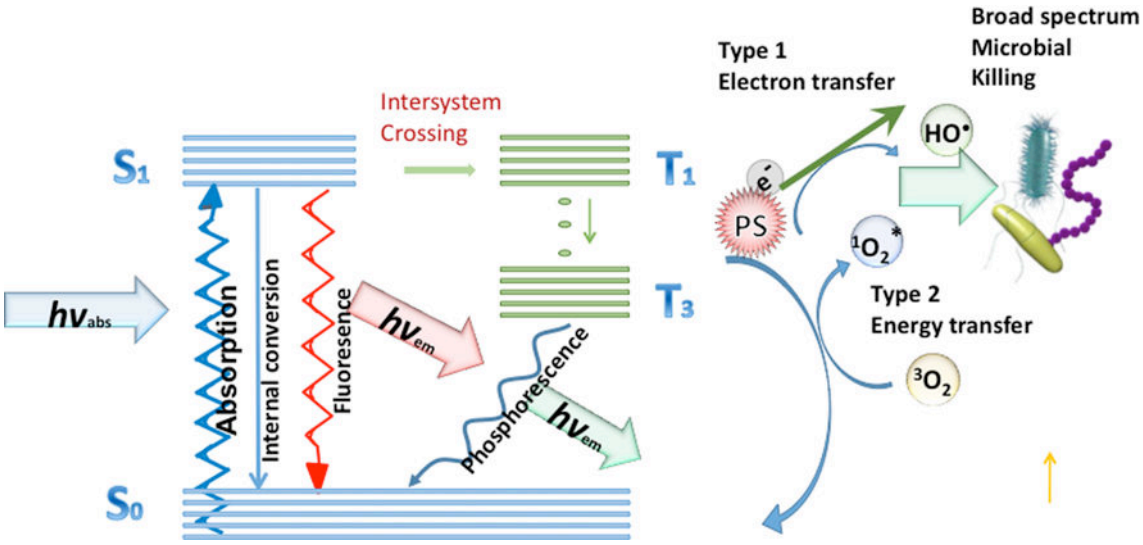

Figure 1. Jablonski diagram

Ground state photosensitizer (^{0}PS) absorbs light to form first excited singlet state (^{1}PS) that (in addition to losing energy by fluorescence or conversion to heat) undergoes intersystem crossing to form the long lived first excited triplet state (^{3}PS). The triplet state can undergo type I (electron transfer) photochemical reaction to form superoxide and hydroxyl radical, and/or type II (energy transfer) photochemical reaction to form singlet oxygen. These ROS can oxidatively damage and kill all known forms of microorganism.

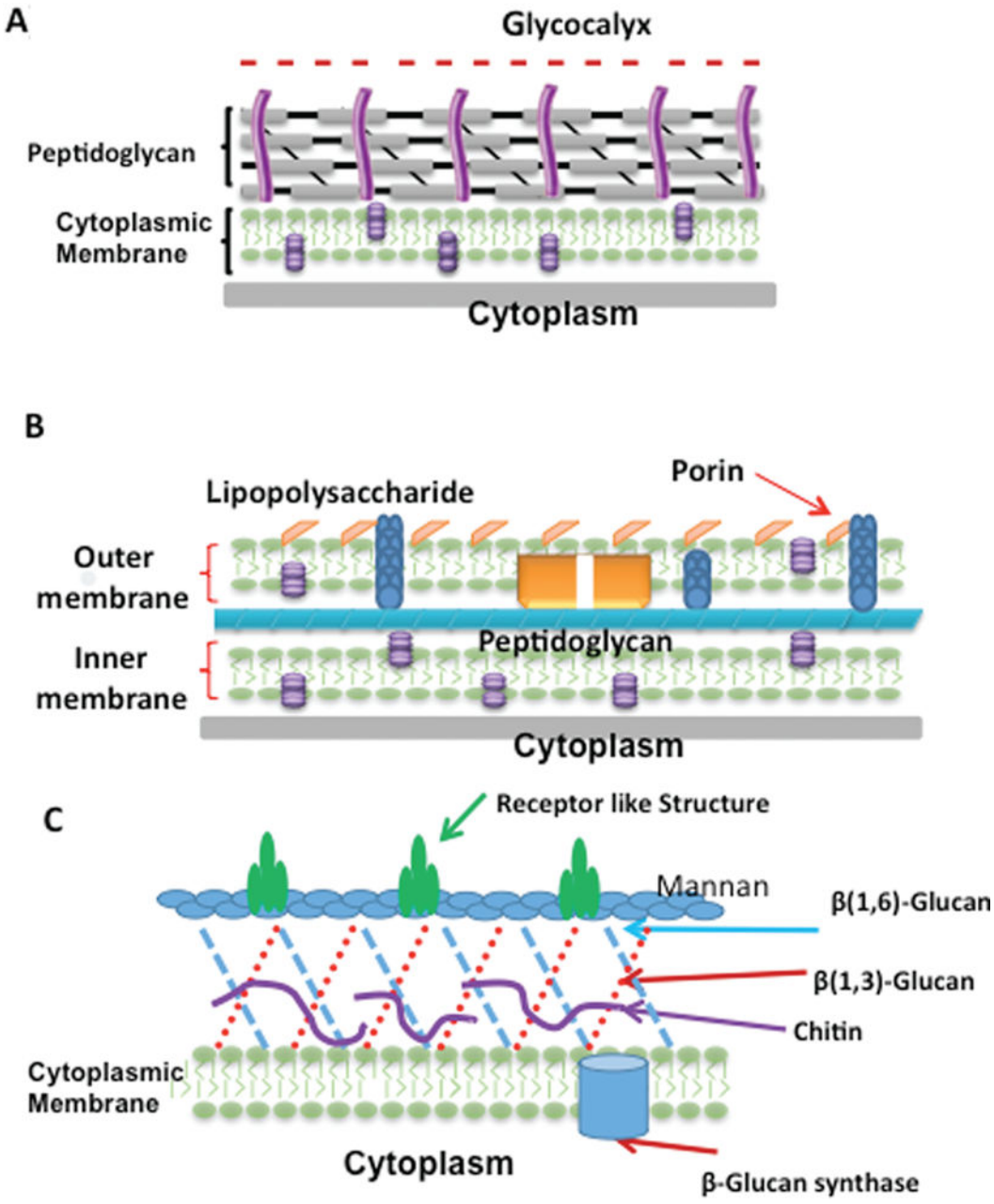

Figure 2. Cell wall structures of Gram-positive and Gram-negative bacteria and fungi

(A) Gram-positive bacteria have a single lipid bilayer surrounded by a thick but porous layer of peptidoglycan, with teichuronic and lipoteichoic acids providing a negative charge. (B) Gram-negative bacteria have a double lipid bilayer (inner and outer membrane) separated by periplasm and peptidoglycan. The outer membrane contains porins and lipoproteins and is decorated with lipopolysaccharide chains with a negative charge. (C) Fungi have an outer cell wall composed of polysaccharides such as mannan, β-glucan, and chitin. The cells do not have a pronounced negative charge and more closely resemble eukaryotic mammalian cells.

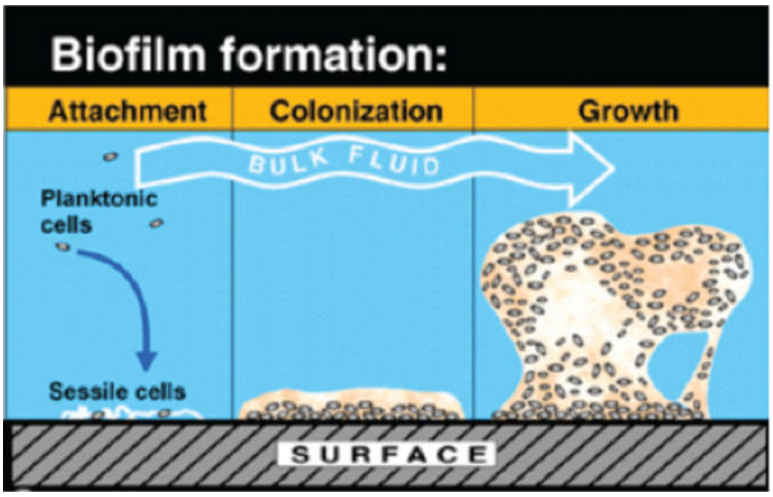

Figure 3. Progression stages of growth of a bacterial biofilm

Initially free-floating planktonic cells settle down onto a surface that can either be inanimate or living tissue. Next secretion of extracellular matrix allows the cells to grow in place. Finally, a mature biofilm is formed complete with water channels to allow oxygen and nutrients to penetrate.

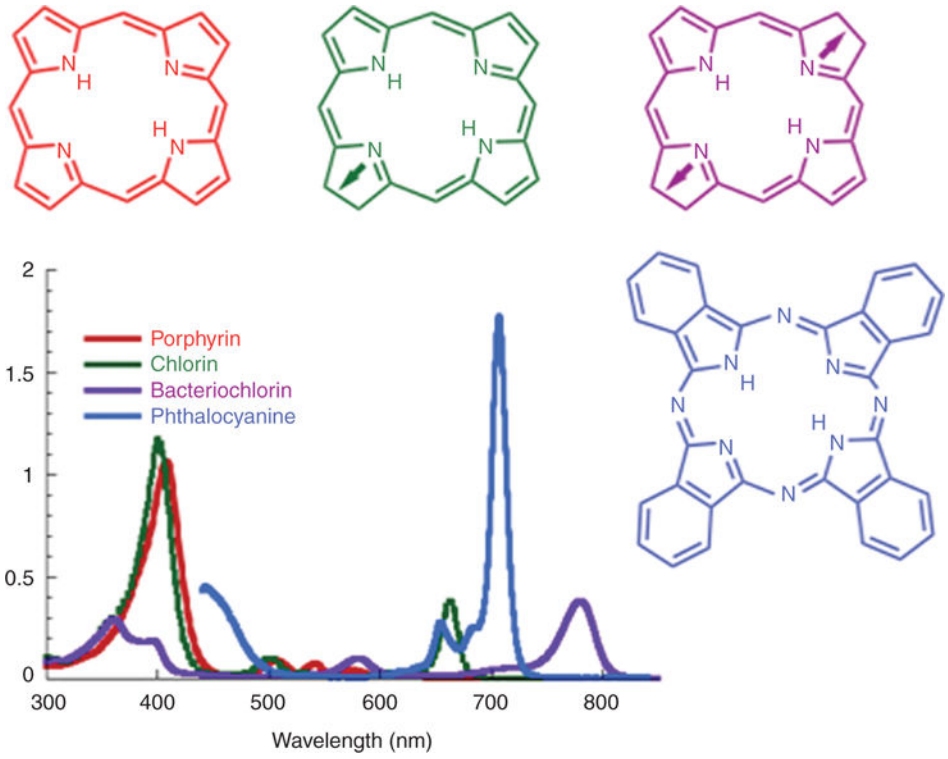

Figure 4. Tetrapyrrole absorption spectra showing porphyrins, chlorins, bacteriochlorins, and phthalocyanines

As pyrrole-ring double bonds are successively reduced starting in porphyrins and going to chlorins and bacteriochlorins, the Q-band moves to longer wavelengths and increases in size.

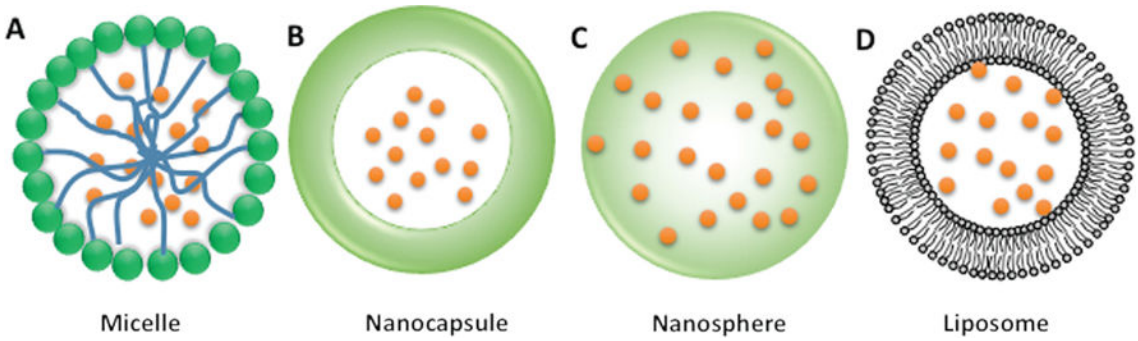

Figure 5. Nanovehicles that have been used to encapsulate PS

Polymeric nanoparticles are sub-μm colloidal particles designed to solubilize hydrophobic PS. (A) Nanomicelles in which amphiphilic co-polymers with hydrophobic and hydrophilic blocks self-assemble to entrap the cargo; (B) nanocapsules, in which the cargo is in solution and surrounded by a shell-like wall; (C) nanospheres, in which the cargo is dissolved, adsorbed, or dispersed throughout the matrix, attached to the surface or attached to the polymer matrix; and (D) liposomes in which an amphiphlic polymer self-assembles into a lipid bilayer that forms a unilamellar vesicle that encapsulates the cargo.

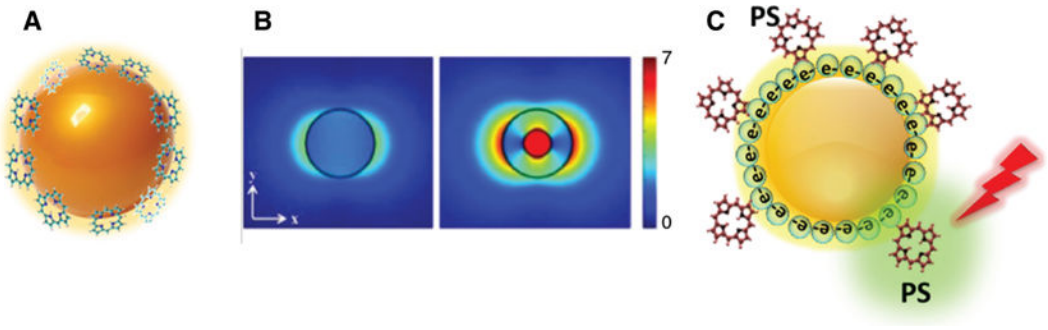

Figure 6. Gold nanoparticle-conjugated PS

(A) Gold nanoparticles with attached PS. (B) Plasmonic gold nanoparticles and nanorings. The local electric field caused by conductance electrons potentiates the optical field close to the surface especially in nanorings. (C) Potentiation of PDT by surface plasmonic enhancement of the photoactivity of an attached PS.

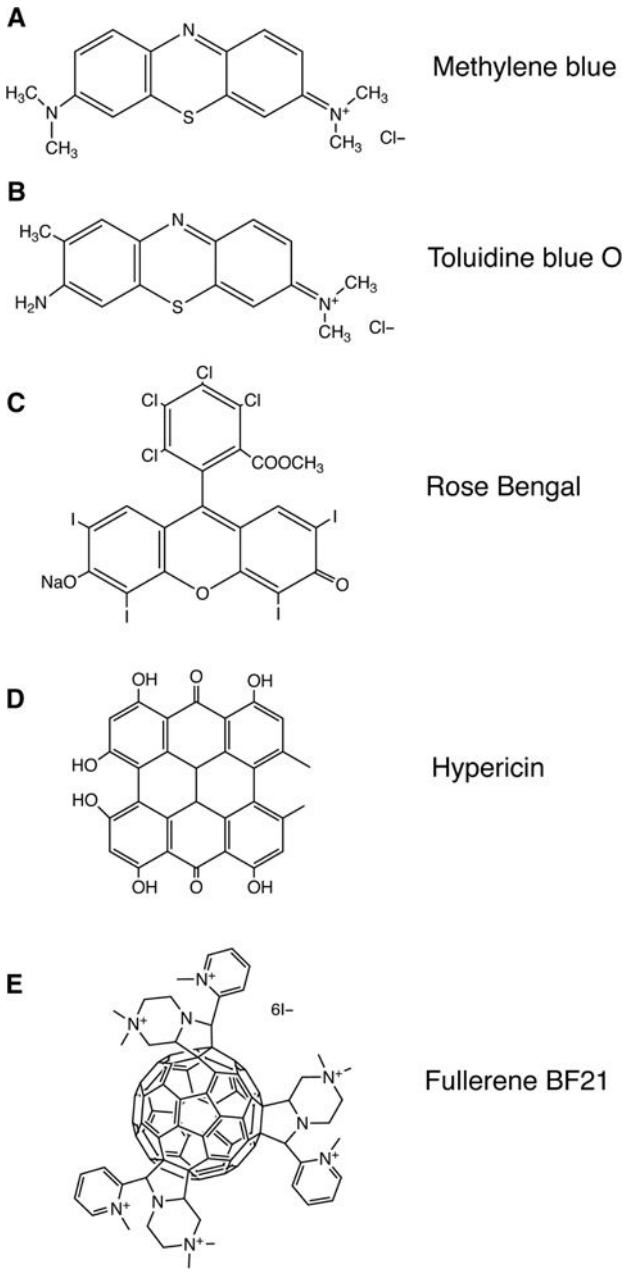

Figure 7. Chemical structures of some PS that have been tested for antimicrobial applications

(A) Methylene blue – a blue phenothiazinium dye. (B) Toluidine blue O – a blue phenothiazinium dye. (C) Rose Bengal – a pink halogenated xanthene dye. (D) Hypericin – a yellow naturally occurring perylenequinone from St John's Wort. (E) BF21 – a brown/black fullerene with six cationic charges.

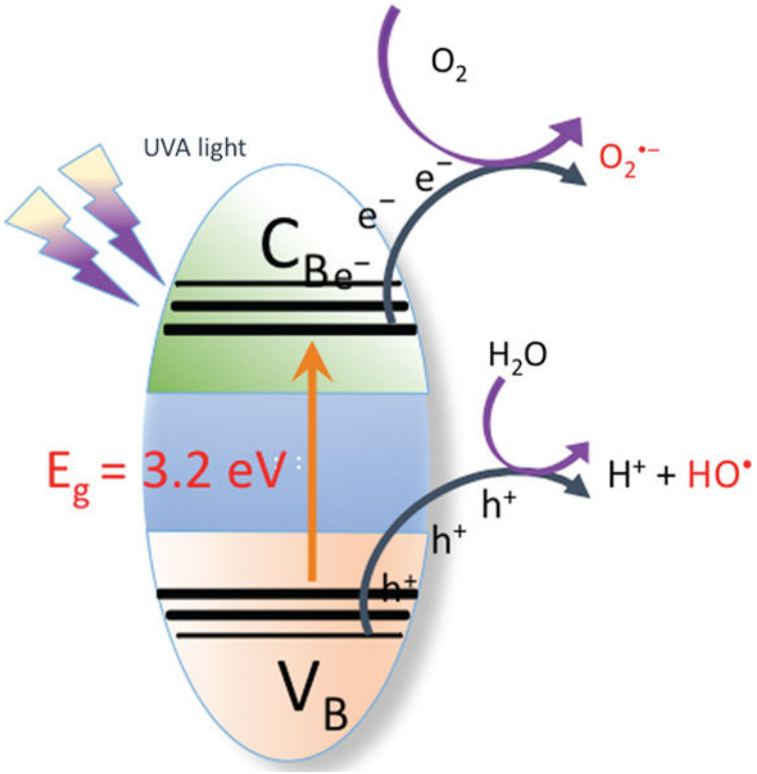

Figure 8. Titania photocatalysis

Schematic illustration of main processes in the photocatalytic reaction of TiO_2. Nanoparticles have a sufficiently large surface area to allow this process to be efficient. Electrons are excited by UVA light from the semiconductor valence band to the conductance band. The electrons in the conductance band undergo electron transfer to oxygen to form superoxide, and the holes in the valence band react with water to form hydroxyl radicals. The ROS produced ($O_2^{\cdot-}$ and HO·) can kill microorganisms.

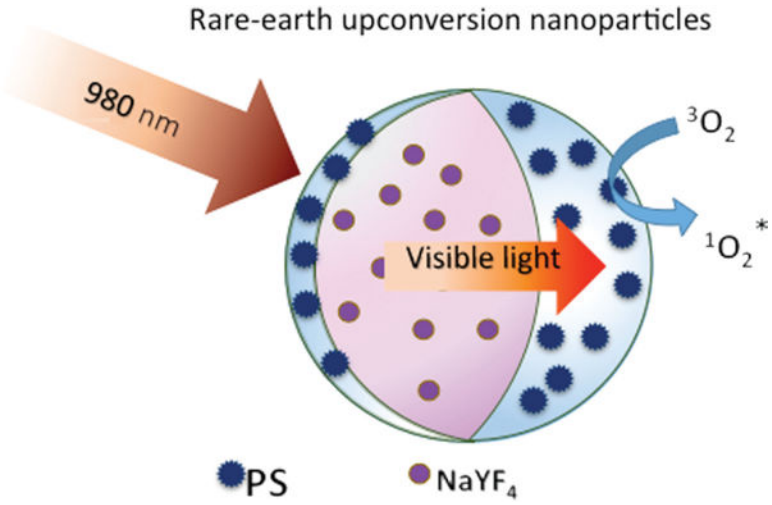

Figure 9. Upconversion nanoparticle-mediated PDT

Nanoparticles made of rare earth salts such as $NaYF_4$ absorb CW 980-nm light and emit short wavelength 400- to 500-nm light that can excite a conjugated PS. Nine hundred and eighty-nanometer light has good tissue penetration but too low energy to excite PS.

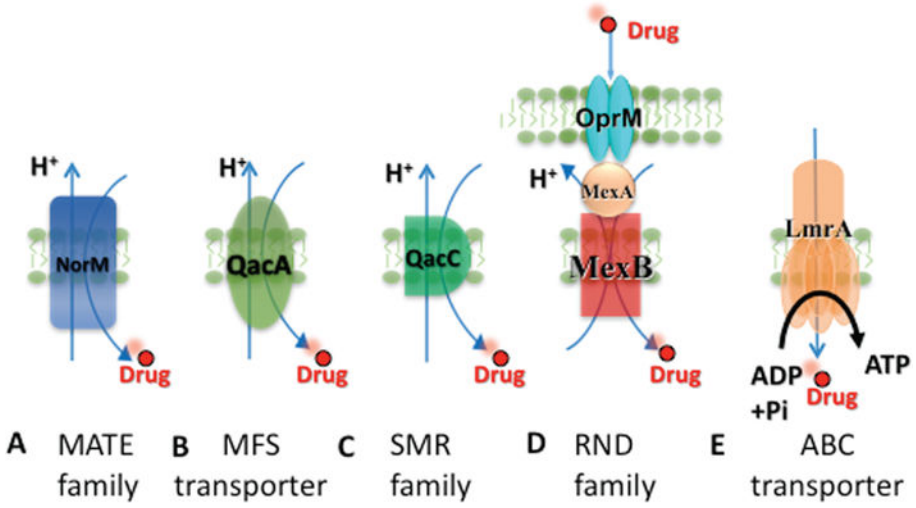

Figure 10. Multi-drug efflux pumps found in various microbial cells

(A) Multidrug and toxic-compound extrusion (MATE) found in both Gram-positive and Gram-negative bacteria. (B) Major facilitator superfam-ily (MFS) found in both Gram-positive and Gram-negative bacteria. (C) Small multidrug resistance (SMR) found in both Gram-positive and Gram-negative bacteria. (D) Resistance nodulation division (RND) found in Gram-negative bacteria. (E) ATP-binding cassette (ABC) transporter found in fungal cells.